State of Oregon
Department of Geology and Mineral Industries
Vicki S. McConnell, State Geologist

Open-File Report O-09-02

PRELIMINARY GEOLOGIC MAP OF THE ROBINSON BUTTE 7.5' QUADRANGLE, JACKSON COUNTY, OREGON

By
Stanley A. Mertzman[1], Stephen G. Weaver[2], Stephen A. Pasquale[3], Jill M. Baum[4], and Isaac P. Weaver[3]

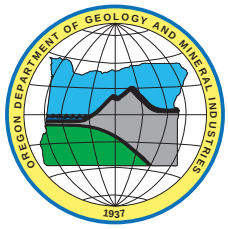

2009

[1]Franklin and Marshall College, Department of Earth and Environment, Box 3003, Lancaster, Pennsylvania 17604
[2]Colorado College, Department of Geology, 14 East Cache La Poudre, Colorado Springs, Colorado 80903
[3]Formerly at Franklin and Marshall College, Department of Earth and Environment, Box 3003, Lancaster, Pennsylvania 17604
[4]Formerly at Carleton College, Department of Geology, Mudd Hall, Northfield, Minnesota 55057

NOTICE

This paper is being published as received from the author(s). No warranty, expressed or implied, is made regarding the accuracy or utility of the information described and/or contained herein, nor shall the act of distribution constitute any such warranty. This disclaimer applies both to individual use of the data and aggregate use with other data. The Oregon Department of Geology and Mineral Industries shall not be held liable for improper or incorrect use of this information.

Oregon Department of Geology and Mineral Industries Open-File Report O-09-02
Published in conformance with ORS 516.030

For copies of this publication or other information about Oregon's geology and natural resources, contact:

Nature of the Northwest Information Center
800 NE Oregon Street #5
Portland, Oregon 97232
(503) 872-2750
http://www.naturenw.org

or these DOGAMI field offices:

Baker City Field Office
1510 Campbell St.
Baker City, OR 97814-3442
Telephone (541) 523-3133
Fax (541) 523-5992

Grants Pass Field Office
5375 Monument Drive
Grants Pass, OR 97526
Telephone (541) 476-2496
Fax (541) 474-3158

For additional information:
Administrative Offices
800 NE Oregon Street, Suite 965
Portland, OR 97232
Telephone (971) 673-1555
Fax (971) 673-1562
http://www.oregongeology.com
http://egov.oregon.gov/DOGAMI/

Introduction

The Robinson Butte 7.5′ quadrangle is located slightly to the west of the present day north-south oriented axis of the High Cascade volcanoes that stretch from British Columbia, Canada to Mount Lassen in northern California. Figure 1 provides exact location information on several levels: the maps indicate where the Robinson Butte quadrangle is situated at the local, south-central Oregon, and Pacific Northwest scales. Topographically the elevation ranges from approximately 2,190 feet where the South Fork of the Little Butte Creek exits the quadrangle flowing to the west, to 5,854 feet, the summit of Robinson Butte, which is located in the northeast corner of the quadrangle, and is its highest point. That means there are 3,664 feet of topographic relief within the Robinson Butte quadrangle. Even though the relief is not excessive, the ruggedness of the valley / canyon incised by the South Fork of the Little Butte Creek dominates the northern half of the quadrangle. In Figure 2A, a photo taken looking south across the upper part of the canyon formed by the South Fork of the Little Butte Creek near the boundary between the Brown Mountain and Robinson Butte quadrangles, the narrowness of the stream valley is quite evident. However, in Figure 2B, a photo taken looking more to the southwest the greater width of the stream valley is easily discerned, and in Figure 2C, looking almost due west, the valley has reached its zenith in terms of width. Given the canyon's increasing width to the west, one can imagine that from above the canyon rim forms the shape of a flat-lying V with its vertex in the east and its two arms extending westward. The local topography is a clear indication that the character of erosion changes dramatically as the South Fork of the Little Butte Creek cuts its channel deeper and deeper into the Miocene Heppsie Formation.

A number of abandoned quarries dot the Robinson Butte landscape. Lava flows and pyroclastics were crushed and used as a source of aggregates for the construction of roads over the past 4 to 5 decades (see Figure 3A, B, and C). Many of these quarries are located within the Heppsie Formation, the oldest rock formation within the Robinson Butte quadrangle. These ~20 Ma igneous rocks are more weathered, fractured, and jointed than the younger volcanic rocks present in the area, and are therefore somewhat less difficult to process into aggregate.

Located at the extreme southern end of the Robinson Butte quadrangle is Howard Prairie Lake, which is part of the Recreational Area System of Jackson County. In 1957-1958 the nearly 30 m high Howard Prairie Dam was constructed on Beaver Creek in the adjacent Hyatt Reservoir quadrangle (see Figure 1). Also, between 1956 and 1959 the Howard Prairie Delivery Canal was fabricated that connects Howard Prairie Reservoir (see Figure 4) with the Keene Creek Reservoir, a small reservoir on Keene Creek below Hyatt Reservoir (in the Links section at the end of this document, the two web sites listed provide a history of irrigation development in the Jackson – Klamath County region). At this small reservoir, flows from Howard Prairie Canal combine with releases from Hyatt Reservoir and the water departs the Klamath basin through the Cascade Divide Tunnel, which connects Keene Creek Reservoir to Emigrant Creek in the Rogue River drainage basin. Much of the surface water in the southeastern quarter of the Robinson Butte quadrangle is diverted through a series of small canals and channels into this water system.

Three paved roads provide access into the Robinson Butte quadrangle. To the north, Lake Creek Road, a dead end road that diverges to the southeast from Oregon State Route

140 as one travels from Medford towards Klamath Falls. It follows the floodplain of the South Fork of the Little Butte Creek and ends where the Dead Indian Creek joins the Little Butte Creek (see Figure 1). Several miles before the road's end is an intersection with the Conde Creek Access road, which from the junction heads south and eventually joins the Dead Indian Memorial Highway that crosses the southern section of the quadrangle and provides much of the traffic into and out of the Howard Prairie Recreation Area. Lastly, in the southeastern corner of the quadrangle the Keno Access road connects the Dead Indian Memorial Highway with Oregon State Route 66 to the south and provides access to Howard Prairie for the people who live in the area to the south of Klamath Falls. On a given summer weekend a number of recreational vehicles will be encountered on all three roads as people travel to Howard Prairie Lake for fishing, boating, and camping activities.

Before embarking on a broad examination of the geology of the Robinson Butte quadrangle, a comment on rock nomenclature is in order. When geoscientists classify igneous rock samples they often come at it from two points of view. One is based on identifying the visible minerals in a hand sample (a modal mineral classification) and the other is based on a chemical analysis of that sample (a chemical classification of igneous rocks – see Figure 5 as an example). Naturally the latter is more precise and rigorous and the former is looser and less precise and is open to more opinions. The most common volcanic rocks (basalt, basaltic andesite, andesite, dacite, rhyolite) define a sequence in which the iron- and magnesium-bearing silicate minerals (olivine, orthopyroxene, clinopyroxene, hornblende, biotite) are most abundant on the left side of the sequence, forming upwards of 50 to 60 percent of the minerals present and decrease to nearly zero to the right, namely, in rhyolite. The remaining 40 to 50 percent of the rock consists mostly of plagioclase feldspar, a non-iron magnesium bearing silicate mineral, plus a few percent of chromium-, iron-, and titanium-dominated oxide minerals. With regard to rock chemistry, silica (SiO_2) increases from basalt to rhyolite and correlates directly with increasing viscosity and greater explosivity.

Table 1, which accompanies the geologic map of the Robinson Butte quadrangle, contains the chemical and age data for all the analyzed rock samples. Figure 1 also depicts the locations of all the samples for which ages exist, both within the Robinson Butte quadrangle and in quadrangles immediately adjacent to it. These adjacent ages are depicted because they are from extensions of the volcanic rock units found within the Robinson Butte map area. The goal was to show all the ages for each volcanic unit discussed in the Explanation of Map Units. Figure 5 is a total alkali ($Na_2O + K_2O$) versus SiO_2 diagram that summarizes the rock names that are most germane for the volcanic materials present in this quadrangle. In addition the chemical data are displayed for each stratigraphic unit that is defined below (except the Qls samples) using an individualized symbol that is summarized in the legend that accompanies Figure 5. Lastly, Mertzman (2000) and Mertzman (unpublished data, 2007 and 2008) provide many new ages, derived from both a whole rock K-Ar method and $^{40}Ar/^{39}Ar$ technology that have been measured through January 2009.

In this region, the older phase of volcanism known as the Early Western Cascade Episode extends from 35 to 17 Ma (late Eocene to the beginning of mid-Miocene time [Gradstein and others, 2004]) while the younger phase of volcanism known as the Late Western Cascade Episode covers the block of geologic time from 16.9 to 7.5 Ma (mid- to late Miocene) (Priest and others, 1983; Priest, 1990). Only where erosion has removed the

veneer of even younger High Cascade volcanic activity is evidence of older volcanic activity apparent. Figure 6 has two parts: the upper portion (6A) is a histogram that summarizes whole rock K-Ar and $^{40}Ar/^{39}Ar$ ages determined solely on rock samples from the Robinson Butte quadrangle. The lower portion of Figure 6 (6B) incorporates all the geochronologic data from the upper diagram with absolute age data from adjoining quadrangles. There is an unconformity (age gap) of 13 to 14 million years magnitude, from essentially 20 to 6 Ma, which characterizes the volcanic activity within the Robinson Butte quadrangle. The Heppsie Formation encompasses all the locally present volcanic material erupted during Early Western Cascade Episode. This age data distribution is significantly different from that reported in the Mule Hill quadrangle farther to the south (Mertzman and others, 2008). In the latter region the Basalt to Andesite of Hayden Creek essentially bisects the unconformity, extending from 15 to 13 Ma. Volcanism of corresponding age is completely missing from the Robinson Butte segment of the Cascade Range.

The South Fork of the Little Butte Creek in the Robinson Butte quadrangle and the Klamath River in the Mule Hill quadrangle have one striking geologic feature in common: landslides. As initially reported by Hazlett and others (1997) and amplified by Mertzman and others (2008), once the Klamath River had eroded down through the unconformable surface described above, it encountered a hundred meters or more of weakly welded silicic pyroclastic rock that forms the youngest segment of the Heppsie Formation. Be aware that in both locations what are situated on top of the unconformable surface are almost exclusively massive mafic lava flows. Once a stream of any magnitude has cut appreciably down into the structurally much weaker pyroclastic material, the stage is set for the development of landslides. This would be especially true at certain times of the year when significant water soaks into the ground and moves downward towards the top of the groundwater table. The added water would further reduce the cohesion along the unconformity, setting the stage for a landslide if a triggering event like an earthquake occurred at the right moment in time. The valley / gorge of the South Fork of the Little Butte Creek deepens and widens quickly from the east side to the west side of the Robinson Butte quadrangle. Landslide scars are numerous on both sides of the creek. Figure 2B provides a broad perspective of the north-facing valley wall that appears scalloped from side-by-side landslide scars. Figure 7 provides a close up image of the headwall area of a relatively young landslide.

The upper portion of the Heppsie Formation consists of the most silicic rock in the region. It is dacite to rhyolite in composition (see Figure 5 and Table 1) and was deposited as part of one or more pyroclastic flow eruptions with their attendant air-fall tephra that was followed by the re-working of the uppermost material by surficial processes. The majority of the Heppsie Formation consists of basalt, basaltic andesite, and andesite lava flows that are abruptly overlain with silicic pyroclastic material with no observable unconformity separating its more mafic component from its more silicic component. Figure 8 depicts columnar jointing in the welded portion of the tuff unit that crops out on the north side of the South Fork of the Little Butte Creek. The photo was taken from the south side of the stream looking to the north. The Short Creek drainage (see geologic map for exact location) provided access to the moderately to intensely welded columnar jointed segment of the pyroclastic flow (see Figure 9A). At this location the welded tuff rests on top of a 3 to 4 m thick columnar jointed basalt flow without a sign of a significant time gap (see sample 00-62). Samples 00-63 through 00-66 are from the lower to the upper-most level (respectively) in the columnar jointed outcrop of welded tuff depicted in Figure 9A. See Table 1 for

sample geochemistry and Figure 5 for a graphic depiction of some of the chemical data. Samples 00-62, 63, and 65 have $^{40}Ar/^{39}Ar$ ages available. Within the limits of precision for each of these analyses the three ages are essentially identical, 21 Ma, which clearly signals they are Heppsie Formation in age. Sample 00-63 is from the columnar jointed part of the outcrop while 00-65 and 00-66 are from the upper 2 m of the outcrop in which the rock is perlitic obsidian in nature; that is, the glassy matrix is partially devitrified, so even though it resembles obsidian, it rather easily breaks apart into pebble-sized fragments. Figure 9B depicts the unsorted and unstratified material that forms the hill slope statigraphically above the pyroclastic flow outcrop. Notice the abundance of pumice and lithic fragments. Much handpicking was involved to collect a lithic-free sample of just pumice fragments that would truly represent the magma component only. In the Willow Lake quadrangle, located immediately north of the Robinson Butte quadrangle (see Figure 1), Oregon State Route 140, which connects Medford to Klamath Falls, Oregon, follows the North Fork of the Little Butte Creek stream valley. The road is located on the north side of the creek itself. The highway right-of-way is wide and cuts through 50 to 100 m of unstratified pyroclastic material identical to that depicted in Figure 9B. Figure 10 provides a broader view of these outcrops along this segment of State Route 140.

Basalt of Pole Bridge Creek (Tmbpb) is an enigmatic volcanic unit. It is part of the initial volcanic activity that constitutes the early phase of Cascade volcanism that commenced between 7 and 6 million years ago in this segment of the Cascade Mountain chain. Lavas poured out onto a land surface that had been undergoing weathering and erosion since the end of the Heppsie Formation volcanic activity nearly 20 Ma before. What makes this unit so unusual is that it is trachybasalt in nature (see Figure 5). The very high alkali element content ($Na_2O + K_2O$), especially the K_2O, together with quite high Sr and Ba concentrations, elements that can often substitute for K in a number of silicate minerals, are chemical characteristics that readily distinguish Basalt of Pole Bridge Creek from any other rock unit between Crater Lake and the California border (see Figure 11A and 11B). Basalt of Pole Bridge Creek lavas can be divided into two groups based on geochemical and petrographic criteria. The precise details are given in the “Explanation of Map Units” section on Basalt of Pole Bridge Creek, but suffice it to say the group with higher MgO and P_2O_5 values also had sufficiently high water pressure values in the last magma chamber in which the molten material resided prior to extrusion on to the Earth’s surface. At depth, this higher water pressure stabilized an amphibole, most likely hornblende in terms of its chemical composition. That one finds amphibole existing together with phenocrystic plagioclase, clinopyroxene, olivine, and an opaque mineral strongly suggests a lower to mid-crust depth for this Basalt of Pole Bridge Creek magma storage chamber. Granular pseudomorphs have replaced the original amphibole as it reacted and dehydrated on its way to the surface.

The latest phase of volcanic activity within the Robinson Butte quadrangle is basaltic in composition and involves two point sources for this volcanism, one within the quadrangle (Robinson Butte) and the other in the Lake of the Woods South quadrangle (Burton Butte), two quadrangles to the east. Although activities at both sources involved diktytaxitic basalt with silica contents ranging between 49 and 52 percent SiO_2, these two basalts are rather easily distinguished on the basis of their hand sample mineralogy. Although both are grayish, spongy textured basalts, Robinson Butte lavas characteristically will have nearly equal amounts of 1 to 2 mm olivine and clinopyroxene phenocrysts that are

easily visible with abundant plagioclase of similar to smaller size, whereas Burton Butte lavas characteristically have 1 to 2 mm olivine phenocrysts with abundant plagioclase that is also similar to smaller in grain size. No clinopyroxene is evident in hand samples of Burton Butte lavas. These observations are borne out with detailed petrographic examination of thin sections. Also, the Robinson Butte lavas invariably have an intergranular texture wherein small olivine and clinopyroxene granules ≤ 0.1 mm in diameter are scattered between laths of plagioclase feldspar. On the other hand the Burton Butte lavas quite often will have a subophitic texture in which the somewhat later crystallizing clinopyroxene molds itself around the margins of the earlier formed plagioclase feldspar laths (rectangles).

Explanation of Map Units

Surficial Units

Qal **Alluvium (Pleistocene to Holocene)—**Unconsolidated sediment found in close proximity to modern drainages. The question mark on the Robinson Butte Map Plate's Time Rock Chart at the base of Qal is to clearly indicate the lack of definitive chronological information with regard to the timing of initial Qal deposition.

Qls **Landslide deposits (Pleistocene to Holocene)—**Unconsolidated volcanic breccia found in close association with the South Fork of the Little Butte Creek, specifically where it has down-cut into Mid-Miocene weakly welded silicic pyroclastic rocks that have relatively thick, massive, mafic lava flows unconformably resting on top of them. Similar geologic circumstances exist further to the south in the Mule Hill quadrangle along the Klamath River (Mertzman and others, 2008) for which Hazlett and others (1997) have suggested that the unconformity is a zone of structural weakness prone to slippage of the massive, dense stack of lavas downhill under the influence of gravity given suitable friction-reducing circumstances (significant rain or melting snows to lubricate this boundary zone) coupled with a triggering mechanism like an earthquake.

The question mark on the Robinson Butte Map Plate's Time Rock Chart at the base of Qls is to clearly indicate the lack of definitive chronological information with regard to the timing of initial Qls deposition.

Volcanic Units

Qbv **Basaltic to basaltic andesite vent deposits (Middle Pleistocene)—**Poorly lithified to unconsolidated lapilli to ash-sized cinders, black to brown to red with lesser amounts of similarly colored lava spatter, bombs, and scoria. These deposits mark volcanic vents areas that are often scoria or cinder cones. The question mark over Qbv in the Robinson Butte Map Plate's Time Rock Chart is there to clearly indicate the lack of definitive chronological information with regard to the timing of initial and final Qbv extrusion.

Qbbb **Basalt of Burton Butte (Middle Pleistocene)—**Light gray to dark bluish-gray in hand sample color, lava samples are consistently lighter in color than that of pyroclastic samples. Burton Butte cinder / scoria cone, the source of these lavas, is located two quadrangles to the east in the Lake of the Woods South quadrangle. Pahoehoe lava flows from Burton Butte spread westward nearly six miles, down the paleo-drainage now occupied by the Beaver Dam Creek all the way to Deadwood Prairie. Most samples have a diktytaxitic (sponge-like) texture (see Figure 12) with a set of large vesicles present, several mm to one centimeter in diameter, that are often lined to partially filled with secondary mineralization, mostly carbonate with some silica and zeolitic minerals infrequently present. The set of larger vesicles is often stretched out to provide a lineation parallel to the last flow direction of the lava. Plagioclase, 0.5 to 2 mm in diameter, is the most abundant mineral, constituting nearly 50 percent of a typical hand sample. Olivine is present as 2 to 3 mm phenocrysts, which exist in glomeroporphyritic clumps, some of which are composed entirely of olivine crystals; others contain plagioclase. Olivine is also present as smaller crystals that range down to groundmass-forming material. Overall, olivine forms 15 to 25 percent of a typical sample. A similar amount of clinopyroxene is present (15 to 25 percent), filling the interstices between the tabular laths of plagioclase with olivine and opaque mineral grains, thus forming an intergranular texture. If cooling was somewhat slower, the clinopyroxene has a chance to form larger crystals that grow around and partially envelope the earlier formed plagioclase crystals, thus forming a subophitic texture (see Figure 13). Chromite, present within early-formed olivine crystals, together with titanomagnetite and ilmenite, are the opaque minerals that constitute 8 to 10 percent of the minerals present in these basaltic lavas. Several whole rock K-Ar ages are available for this unit, none from the Robinson Butte quadrangle, and are characterized by relatively large uncertainties. These relatively large error limits are due in part to the low whole rock K_2O values for the Burton Butte basalt samples, < 0.3 percent, coupled with its young age. One $^{40}Ar/^{39}Ar$ age has been quite recently determined on a sample from the Brown Mountain quadrangle (see sample 91-5) and is preferable over all the others. Burton Butte volcanic activity is 0.33 ± 0.12 Ma old.

Qbrb **Basalt of Robinson Butte (Middle Pleistocene)—**Light gray to dark bluish-gray in hand sample color, lava samples are consistently lighter in color than that of pyroclastic samples. Robinson Butte cinder / scoria cone, the source of these lavas, is located in the extreme northeast corner of the Robinson Butte quadrangle. Two views of Robinson Butte are provided in Figure 14A and B. Three to five meter thick lava flows with pahoehoe surfaces are abundant. Vesicles 5 to 10 mm long, stretched out in the direction of flow and partially lined with vapor-phase-deposited secondary minerals, are common. The lava flows are only vaguely diktytaxitic in nature, most likely due to the slightly higher silica content (~50 to 52 percent SiO_2) than Burton Butte lavas that quite often display well developed diktytaxitic texture. The lavas have a glomeroporphyritic texture with olivine (1 to 3 mm in maximum dimension), often distinctly rimmed with low temperature iddingsite alteration, constituting 10 to 15 percent of each hand sample (see Figure 15). Poikilitic within early-formed olivine crystals are chrome-spinel inclusions (see Figure 15). Abundant clinopyroxene (1 to 3 mm) and plagioclase (0.5 to 1 mm) phenocrysts constitute nearly 50 percent of a hand sample and are present in glomeroporphyritic clumps as well as individual crystals (see Figure 16). Several per cent of the plagioclase phenocrysts present in the Robinson Butte basaltic lavas have a strikingly different appearance than the vast majority of plagioclase crystals in that the crystals have been strongly resorbed into a fine grained

crystalline aggregate that have thin rims of unaltered later-formed plagioclase (see Figure 17). These severely altered phenocrysts could be xenocrysts, that is, foreign crystals entrained by the rising Robinson Butte magma on its way to the surface. The groundmass is primarily intergranular to subophitic in nature. One whole rock K-Ar age is available for this unit, 0.40 ± 0.30 Ma, measured on a sample from the easterly adjacent Brown Mountain quadrangle. One $^{40}Ar/^{39}Ar$ age has been quite recently determined on sample 00-67 from the Robinson Butte quadrangle and is preferable because of its much better precision. Robinson Butte volcanic activity is 0.36 ± 0.06 Ma old. From a geologist's point of view it is very interesting to note that the volcanic activity at Robinson Butte and Burton Butte are virtually identical in age, which suggests these two volcanoes could have simultaneously been erupting basaltic lava onto the southern Oregon landscape. As the chemical compositions of basaltic lavas from Robinson and Burton Buttes are easily distinguishable, one implication is that the plumbing systems for each of these two volcanoes are separate and distinct.

Tpbbm Basalt of Brush Mountain (Upper Pliocene)—The Brush Mountain volcanic vents are aligned in a NNW-SSE direction in the extreme south-central part of the Brown Mountain quadrangle and extend into the Little Chinquapin Mountain quadrangle. Numerous basaltic lava flows are found in both quadrangles that emanate from these linearly arrayed vents. Brush Mountain basalts are medium gray as lavas and considerably darker gray as the lavas become more vesicular in nature. These extrusive rocks are porphyritic with plagioclase feldspar somewhat more abundant than olivine in phenocrysts that compose 10 to 15 percent of the basalts. These two minerals occur separately and in glomeroporphyritic clumps that can range up to 3 mm in diameter. Pyroxene is mostly confined to the matrix. The olivine is partially altered to iddingsite, a characteristic that causes the olivine phenocrysts to be much more darkly colored than the typical lime green; it also causes olivine to be iridescent, particularly in shades of purple on newly broken surfaces. Two whole rock K-Ar ages are available for this unit, 2.22 ± 0.12 Ma and 1.97 ± 0.08 Ma old (94-14 from the Little Chinquapin Mountain quadrangle and 94-16 from the Brown Mountain quadrangle, respectively). There is only a small sliver of Basalt of Brush Mountain in the southeast corner of the Robinson Butte quadrangle; its area is approximately 0.005 km^2.

Tpbmp Basalt of Moon Prairie (Lower Pliocene)—These mostly olivine-phyric lavas form the far southeast corner of the map area and have flowed from fissure-like vents from which all the capping pyroclastic material has been eroded away. Several of these fissure / very shallow dikes are found in the area and are marked by vertically aligned flow-jointed linear features that are several tens of meters to more than 100 m long. In addition to olivine-phyric lavas there are also interspersed flows that have olivine and clinopyroxene phenocrysts (see Figure 18), with plagioclase confined to mostly a groundmass status, as well as flows that are substantially more granular wherein phenocrysts of plagioclase, olivine, and clinopyroxene are readily identified. Part of the petrographic variability arises from comparing lava flows (or parts therein) that cooled at different rates. However, changing the sequence of mineral crystallization from spinel – olivine – clinopyroxene to spinel – olivine – plagioclase requires a somewhat different bulk composition as opposed to simple cooling rate changes. Spheroidal weathering is encountered at most of the outcrops of this unit. Olivine forms 15 to 20 percent of a hand sample as phenocrysts 1 to 4 mm in diameter, many of which are partially to completely altered to iddingsite. Numerous small grains of spinel are poikilitically enclosed within the olivine crystals, some of which have

been partially altered to serpentine (see Figure 19). Plagioclase feldspar is the most abundant mineral present but is often confined to the matrix as elongate rectangular crystals (laths) that are flow aligned to produce a trachytic texture (see Figure 20). Present as microphenocrysts and small-sized crystals, clinopyroxene is the only readily identifiable pyroxene present in these light gray basaltic lavas. One $^{40}Ar/^{39}Ar$ age is available for this unit, 4.51 ± 0.01 Ma and comes from sample 99-14 located in the Brown Mountain quadrangle.

Tmbab Basaltic Andesite of Beaver Dam Creek (Upper Miocene to Lower Pliocene)—This unit is stretched across the west-central portion of the Brown Mountain quadrangle and the east central portion of the Robinson Butte quadrangle. Similar to the Basalt of Moon Prairie described immediately above, spheroidal weathering is the order of the day when it comes to examining outcrops of this unit. Nearly every outcrop has one or more very good examples of this weathering phenomenon. Individual rounded boulders commonly display distinctive weathering rinds when broken open, with the most intensively weathered material near the outside surface of the sample becoming less intensively weathered as one penetrates further into the rock mass. This unit has a majority of lavas that are basaltic andesite in composition; however, there are minor but persistent basaltic lavas present as well. These light gray basalts are consistently of the olivine-phyric type with the flow aligned phenocrysts of olivine ranging from 2 to 4 mm in length and constituting nearly 20 percent of the volume of a hand sample. Many of these olivine crystals have been partially to substantially altered to iddingsite (see Figure 21). One memorable occurrence is located north of Shell Rock Butte in the Robinson Butte quadrangle in which olivine phenocrysts 3 to 6 mm in diameter have accumulated in a lava flow so that the modal content is approximately 30 to 35 percent of the rock mass. The whole rock MgO contents for these samples (see samples 94-42, 07SM-20 and 21 in Table 1) are in excess of 15 percent, which is 4 percent higher than any other value measured for samples from the Cascade Mountains of southern Oregon. Compared to these basaltic lavas, the flows of basaltic andesite have fewer phenocrysts and contrary to expectations, given their higher silica content, are much darker bluish-gray. Plagioclase feldspar and olivine phenocrysts, 1 to 3 mm in diameter, constitute 3 to 5 percent of a hand sample's volume and are nearly equal in abundance. Pyroxene and much additional plagioclase are confined to the sample matrix that is much finer grained than in the basaltic lavas. Hence, when breaking the basaltic andesite lava in to smaller chunks, conchoidal fracture surfaces are very abundant. Five whole rock K-Ar ages are available for this unit, 94-42 and 94-40 **(**5.54 ± 0.15 Ma and 5.43 ± 0.18 Ma, respectively) are located in the Robinson Butte quadrangle, while samples 91-43, 91-46, and 91-44 (5.82 ± 0.17 Ma, 5.08 ± 0.13 Ma, and 4.60 ± 0.34 Ma, respectively) are from the adjoining Brown Mountain quadrangle. One $^{40}Ar/^{39}Ar$ age is available for this unit, 5.99 ± 0.04 Ma, and is from sample 07SM-16 from the Robinson Butte quadrangle. Thus, the full range of the radiometric ages for the Basalt Andesite of Beaver Creek extends from 5.99 ± 0.04 to 4.60 ± 0.34 Ma.

Tmbpb Basalt of Pole Bridge Creek (Upper Miocene to Lower Pliocene)—The Basalt of Pole Bridge Creek outcrops rather spectacularly in the region near the confluence of Beaver Dam Creek, Pole Bridge Creek, and the South Fork of the Little Butte Creek in the extreme west-central portion of the Brown Mountain quadrangle. On the east side of the intersection the bluffs are held up by basalt lava flows and are capped by younger basaltic andesite lavas. Individual bluffs have relief ranging from 35 to 60 m. The maximum

thickness of the Basalt of Pole Bridge Creek is on the order of 70 to 80 m. It thins rapidly to the west so that in the Short Creek drainage in the Robinson Butte quadrangle, 2 to 2.5 km further to the west, the Basalt of Pole Bridge Creek has thinned to zero and the 0.4 Ma old Robinson Butte Basalt lies directly upon early Miocene volcanic rocks of the Heppsie Formation. A second patch of Basalt of Pole Bridge Creek lava crops out on the southwest flank of Robinson Butte. A Middle Pleistocene basalt lava flow from Robinson Butte cuts a major expanse of Basalt of Pole Bridge Creek into two segments as it flowed down the Short Creek drainage. On the outcrop, lava flows range from platy jointed near the bases of the flows, with individual plates 1 to 3 cm thick, to essentially massive in the interiors. Individual hand samples are light gray and often possess two generations of vesicles. The first generation of vesicles is larger, forming spherical to oval shaped voids that are 0.2 to 0.5 cm diameter. The second generation of vesicles is pinhead in size and spherical in shape. Both vesicle types are quite fresh; that is, both are unfilled and unlined by secondary minerals in most locations. Inspection of Table 1 indicates that based on whole rock chemistry there are two varieties of Basalt of Pole Bridge Creek. One is has higher concentrations of K_2O, Sr, and Ba while the second is richer in MgO, P_2O_5, and Nb with lesser amounts of K_2O, Sr, and Ba. Most of the Basalt of Pole Bridge Creek samples plot as trachybasalts (see Figures 5, 11A, and 11B), a characteristic that makes these basaltic lavas quite unusual and distinctive when compared to other basalts, for example, those erupted from either Robinson Butte or Burton Butte. Comparatively speaking, these latter basalts have much lower concentrations of the large ionic lithophile elements P_2O_5, K_2O, Sr, and Ba and are quite representative of other diktytaxitic textured basalts present in the Oregonian Cascade Mountains (Hughes, 1990). Cascade lavas with similar K_2O, Sr, and Ba concentrations occur at Goosenest volcano (see Mertzman, 1992), but these Early Holocene lavas are significantly higher in silica and lower in P_2O_5 than the Basalt of Pole Bridge Creek lavas. Also unusual is both the size and abundance of clinopyroxene crystals, in this case equal to or greater than olivine. Many basalts of similar silica content from this region of the Cascades are dominated by olivine, with clinopyroxene relegated to a microphenocryst and / or matrix constituent (Smith and Carmichael, 1968; Hughes, 1990; Leeman and others, 1990). Basalt of Pole Bridge Creek lava flows range from nearly aphyric, that is, phenocryst-free, to containing 20 to 25 percent small phenocrysts ranging between 1 and 2 mm in maximum dimension and consisting of, in order of decreasing abundance, plagioclase, clinopyroxene, olivine, and opaque minerals, a description that fits very well the Group 1 Basalt of Pole Bridge Creek lavas (higher K_2O, Sr, and Ba) identified above. Figure 22 clearly depicts the abundant plagioclase and clinopyroxene phenocrysts with lesser amounts of olivine. Analogous to the clinopyroxene, the opaque minerals are unusually abundant in Basalt of Pole Bridge Creek lavas (10 to 12 percent of total mineralogy) and crystallized early as evidenced by their inclusion within all the silicate minerals listed above (see Figures 23A and 23B). This abundance of relatively early-formed titanomagnetite crystals suggests a greater abundance of Fe^{+3}, which is likely a product of higher oxygen fugacity in the parental Basalt of Pole Bridge Creek magmas (McBirney, 2007). Group 2 of the Basalt of Pole Bridge Creek lavas, those with higher MgO and P_2O_5 coupled with lower K_2O, Sr, and Ba concentrations, have an additional mineral present that is really only noted in thin section. Figure 24 shows two prominent phenocrysts that have been resorbed and the original mineral replaced by a granular aggregate of very small grains dominated by an opaque mineral. Both olivine and clinopyroxene phenocrysts that are only a millimeter or two away from the totally replaced phenocrysts (pseudomorphs) are in pristine form, with no sign of alteration. The shape of the pseudomorph depicted in Figure

25 suggests that the precursor to the granular aggregates was an amphibole, perhaps hornblende. The presence of amphibole pseudomorphs indicates a higher PH_2O, which is required to stabilize a hydrous mineral like hornblende. Although they are infrequently encountered, Mertzman (2000) has noted several examples of amphibole pseudomorphs—in each case the parental extrusive rock is more siliceous in nature, ranging from basaltic andesite to andesite. One last petrographic observation that reflects both compositional groups of Basalt of Pole Bridge Creek lavas is the widespread distribution of groundmass, iron-rich biotite (see Figure 26). This mineral was the last one to crystallize in these lavas and it is likely that it formed via sublimation (McBirney, 2007). Four whole rock K-Ar ages, three from Robinson Butte quadrangle samples (92-21, 6.13 ± 0.10 Ma; RSP94-94, 5.73 ± 0.15 Ma; and JB91-56, 5.35 ± 0.09 Ma) and one from the Brown Mountain quadrangle (RSP-131, 6.14 ± 0.15 Ma), have been determined on Basalt of Pole Bridge Creek samples. One $^{40}Ar/^{39}Ar$ age is available for this unit, 4.35 ± 0.04 Ma, and is from sample 99-5 from the Brown Mountain quadrangle. Thus, the full range of the radiometric ages for the Basalt of Pole Bridge Creek extends from 6.14 ± 0.15 to 4.35 ± 0.04 Ma.

Tmvhf Heppsie Formation[*] (Lower Miocene)—The Heppsie Formation constitutes the youngest portion of the Little Butte Volcanic Series. In this segment of the Formation's outcrop area the older extrusive rocks are dominated by basalt, basaltic andesite, and andesite lava flows, whereas in the younger, upper portion, poorly to intensely welded pyroclastic flow and air-fall tuffaceous material dominate. These latter extrusive materials range from andesite to dacite to rhyolite in terms of their bulk composition. On the outcrop the lavas are greenish-brown in surface coloration, often with several meters or more of soil developed in situ. The most abundant mineral present in these lavas is the nonferromagnesian mineral plagioclase feldspar. It is often unaltered, but in numerous locations it is cut by small cracks and veins filled by sericite mica and calcite plus a little quartz (?). In the more mafic lava flows of this formation, the ferromagnesian minerals, olivine and pyroxene, have reacted very differently to changing physical and chemical conditions. Whereas olivine has quite often been totally converted to iddingsite as a result of relatively low temperature oxidation and hydration, pyroxene has been quite stable and shows little if any sign of alteration. As described in the introduction, the Short Creek drainage, as it incises into the north-side valley wall of the South Fork of the Little Butte Creek, has exposed in a rather dramatic way the stratigraphy of the upper-most segment of the Heppsie Formation. Let's explore the section microscopically by examining a series of photomicrographs. Sample 00-62 is at the base of the exposed section that is several meters of rather typical columnar basalt. Olivine phenocrysts have been converted to iddingsite (see Figure 27) that are enveloped in a fine-grained matrix of plagioclase feldspar laths and clinopyroxene crystals that are essentially unaltered. Directly atop the columnar basalt without any manifestation of a time gap, samples 00-63 through 66 provide a cross-sectional view through either a peculiarly zoned pyroclastic flow or two separate pyroclastic flows separated by an unconformity for which there is little physical evidence (Fisher and Schmincke, 1984). To the north in the Willow Lake quadrangle there is some geochronologic evidence that suggests the less silica-rich basal segment is older (see

[*] **The upper portion of the Heppsie Formation is a poorly to moderately welded pyroclastic flow unit and is mixed in with the base of the landslide deposits along several miles of the South Fork of the Little Butte Creek in the Robinson Butte quadrangle. The Heppsie Formation is an integral part of the Qls formation.**

Table 2 below, sample 02SM-8A) and the more silica-rich upper segment is younger (see Table 2 below, sample 02SM-42). In many instances of chemically zoned pyroclastic flows, the lower portion is more silica-rich and the upper portion is less silica-rich, the exact situation one encounters at Crater Lake, Oregon (Williams, 1942; Beacon and Druitt, 1988). Such a chemical zonation on the outcrop is easy to visualize if one invokes the sequential emptying of a somewhat stratified magma chamber that has been formed through phenocryst fractionation and assimilation of wall rock somewhere within the mid- to upper levels of the crust. Samples 00-63 and 64 are from the poorly to moderately welded section of the flow in which pumice fragments retain much of their original shape and have not been highly modified. Figure 28 provides a representative view of the pyroxene – plagioclase mineralogy; both orthopyroxene and clinopyroxene have been identified, thus making the most appropriate rock name, given its whole rock chemistry (see Table 1), a two pyroxene basaltic andesite to andesite ash-flow tuff. If hydrous minerals like hornblende and / or biotite were ever present in this unit at this location, no conclusive petrographic evidence has yet been discovered. Samples 00-65 and 66 provide a view either into the more intensely welded portion of a singular pyroclastic flow (not as likely) or into the second, upper-most pyroclastic flow that is more silica-rich. Figure 29 is a low magnification image that depicts several percent of scattered small phenocrysts, mostly plagioclase, and vesicles that are stretched out in the direction of flow. Figure 30 provides a close view of a euhedral plagioclase phenocryst that contains an included crystal of earlier formed apatite situated in a matrix of flattened shards of pumice that define flowage lines around the plagioclase crystal. One characteristic of the vesicles associated with pyroclastic flows is vapor-phase crystallization around the vesicle walls. The usual mineralogy is that of quartz and alkali-feldspar (Philpotts, 1989). Figure 31 depicts such a texture. Highly flattened pumice fragments are one of the salient characteristics of intensely welded tuff. Figure 32 documents such an occurrence and Figure 33 depicts intense flowage around a glomeroporphyritic clump of pyroxene, plagioclase, and an opaque mineral, most likely titanomagnetite. Phenocrysts that are in equilibrium with the surrounding magma at the time the magma begins to rise for its extrusion onto the earth’s surface often show the effects of that trip. The magma often heats up as a result of the decompression, and as a result the phenocrysts are no longer in equilibrium with the magma, so they begin to react with it. A cuspate interface results from such a chemical reaction; the once sharp linear boundary surface between the mineral and the magma takes on a seriated knife-like appearance as the mineral dissolves preferentially at certain locations (see Figure 34).

Where the ash-flow tuff member of the Heppsie Formation has been exposed by erosion and due to its inherent structural weakness, numerous landslides and slumps have their beginning at or near the contact between younger more massive basaltic lava flows and the older poorly welded ash-flow tuffs. In the Robinson Butte quadrangle several good examples of arcuate headwall slump structures can be easily found in the canyon of the South Fork of the Little Butte Creek. As one road-building civil engineer said to me (S.A.M.) two summers ago while working on a bridge replacement project across the South Fork, “Nothing in this valley is actually stable. Everything is moving downhill pretty fast, particularly in the spring as the winter snows melt.” Also, numerous excellent examples of landslides / slump development can be found in the Mule Hill quadrangle (Mertzman and others, 2008) in the Klamath River canyon along the California–Oregon border beginning just below the John C. Boyle Powerhouse at what is known as the Caldera Rapid. In this region a very similar layering of geologic rock units occurs as in the South Fork of the Little

Butte Creek: older siliceous poorly welded tuffaceous material is overlain by younger, thick occurrences of mafic lava flows. It is likely that the same mechanism of slope failure is occurring in both areas, giving rise to landslides / slumps that set the stage for rapids to form in the streams that are flowing through the valleys. Thirteen ages for various Heppsie Formation samples, both whole rock K-Ar and $^{40}Ar/^{39}Ar$ ages, are available from the general area north of the Klamath Falls–Ashland highway, State Route 66. A summary of the geochronology available from samples my team and I have collected over the years is provided in Table 2. The ages from the United States Geological Survey in Denver, abbreviated USGS below, and New Mexico Institute of Mining and Technology, abbreviated NMT below, are $^{40}Ar/^{39}Ar$ ages. The age dates that I determined at Case Western Reserve University, abbreviated CWRU below, are whole rock K-Ar samples. Since the K-Ar whole rock ages are more susceptible to alteration and weathering processes (notice that most Heppsie Formation K-Ar ages are ≤ $^{40}Ar/^{39}Ar$ ages), the $^{40}Ar/^{39}Ar$ data is much more likely to be accurate (Faure, 1986).

Table 2. Compilation of Heppsie Formation radiometric age dates. An [a] indicates a $^{40}Ar/^{39}Ar$ date; all other dates were determined by the K-Ar dating method.

Sample #	Age (Ma)	Source	Quadrangle
00-65	21.1 ± 0.3[a]	USGS	Rob. Butte
00-63	21.2 ± 0.3[a]	USGS	Rob. Butte
00-62	21.10 ± 0.07[a]	USGS	Rob. Butte
91-61	19.6 ± 0.3	CWRU	Rob. Butte
92-24	20.5 ± 0.3	CWRU	Rob. Butte
92-26	20.2 ± 0.3	CWRU	Rob. Butte
92-41	19.5 ± 0.3	CWRU	Rob. Butte
07SM-3	21.49 ± 0.10[a]	NMT	Rob. Butte
07SM-10	20.4 ± 0.3[a]	NMT	Rob. Butte
02SM-8A	21.15 ± 0.08[a]	USGS	Willow Lake
02SM-42	19.93 ± 0.07[a]	USGS	Willow Lake
03SM-21	21.73 ± 0.14[a]	NMT	Hyatt Res.
03SM-11	22.27 ± 0.13[a]	NMT	L. Chinquapin Mtn.

Acknowledgments I thank Isaac Weaver for his on-going help and cheerful support in bringing this geologic map to closure. His computer skills, particularly with regard to MapInfo and Adobe Illustrator, have been particularly valuable. I also thank Karen Mertzman for all her efforts in the X-ray lab, carefully preparing and analyzing countless samples on my behalf. I thank the Keck Foundation for its generous support of the Keck Geology Consortium over the years. I thank Franklin and Marshall College for its generous support of fieldwork over the past decade that has led to the completion of this geologic map. Support from the NSF and Franklin and Marshall College to facilitate the operation of the XRF laboratory in the Earth and Environment Department is greatly appreciated.

Links

http://www.talentid.org/mn.asp?pg=DistrictHistory

http://www.usbr.gov/dataweb/html/rogueriver.html

References

Baker, I. and Haggerty, S. E., 1967, The alteration of olivine in basaltic and associated lavas, Part II: Intermediate and low temperature alteration, Contr. Mineral. Petrol. v. 16, 258-273.

Beacon, C. R. and Druitt, T. H. 1988, Compositional evolution of the zoned calcalkaline magma chamber of Mount Mazama, Crater Lake, Oregon, Contr. Mineral. Petrol. V. 98, 224-256.

Faure, G., 1986, *Principles of Isotope Geology, 2nd Edition*: New York, John Wiley & Sons, Inc., 589 p.

Fisher, R. V. and Schmincke, H. -U., 1984, *Pyroclastic Rocks*, Berlin Heidelberg, Springer Verlag, 472 p.

Gradstein, F., Ogg, J., and Smith, A. ed. 2004. *A Geologic Time Scale 2004.* Cambridge, Cambridge University Press, 589 p.

Haggerty, S. E. and Baker, I., 1967, The alteration of olivine in basaltic and associated lavas, Part 1: high temperature alteration, Contr. Mineral. Petrol., v. 16, 233-257.

Hazlett, R., Bilstrom, E., Cross, B., Kormeier, G., and Mertzman, S, 1997, Widespread Late Pleistocene Landsliding Event in the Area of Secret Spring Volcano, Southern Oregon Abstracts with Program 1997 Geological Society of America Meeting, Salt Lake City, Utah.

Hughes, S. S., 1990, Mafic magmatism and associated tectonism of the Central High Cascade Range, Oregon, Jour. Geophy. Res. v. 95, no. B12, 19623-19638.

Le Maitre, R. W. ed. 2002. *Igneous Rocks: A Classification and Glossary of Terms.* 2d ed. Cambridge: Cambridge University Press, 252p.

Leeman, W. P., Smith, D. R., Hildreth, W., Palacz, Z., and Rogers, N., 1990, Compositional diversity of Late Cenozoic basalts in a transect across the southern Washington Cascades implications for subduction zone magmatism, Jour. Geophy. Res., v. 95, no. B12, 19561-19582.

McBirney, A. R., 2007, *Igneous Petrology, 3rd Edition*, Boston, Jones and Bartlett Publishers, 550 p.

Mertzman, S. A., 1992, Goosenest volcano, southern Oregon: High K_2O, Ba, and Sr basaltic andesite extrusives: GSA Annual Mtg. Abstracts with programs, v. 24, no. 7, A262.

Mertzman, S. A., 2000, K-Ar results from the southern Oregon-northern California Cascade Range, Oregon Geology, v. 62, 99-122.

Mertzman, S. A., and others 2008, Preliminary Geologic Map of the Mule Hill 7.5' Quadrangle Klamath County, Oregon and Siskiyou County, California. Open File Report #O-08-08.

Neese, W. D., 2004, *Introduction to Optical Mineralogy, 3rd Edition*, New York, Oxford University Press, 348p.

Philpotts, A. R., 1989, *Petrography of Igneous and Metamorphic Rocks*: Illinois, Waveland Press, Inc, 178p.

Priest, G. R., 1990, Volcanic and tectonic evolution of the Cascade volcanic are, central Oregon, J. Geophys. Res. *v.* 95, 19583-19599.

Priest, G. R., Woller, N. M., Black, G. L., and Evans, S. H., 1983, Overview of the geology of the central Oregon Cascade Range, Geology and Geothermal Resources of the Central Oregon Cascade Range, edited by G. R. Priest and B. F. Vogt, Spec. Pap. Oreg. Dep. Geol. And Miner. Ind., v. 15, 3-28.

Rogue River Basin Project: Talent Division - Oregon. Last accessed on March 24, 2009: <http://www.usbr.gov/dataweb/html/rogueriver.html>.

Smith, A. L., and Carmichael, I. S. E., 1968, Quaternary lavas from the southern Cascades, western U. S. A., Contr. Mineral. Petrol., v. 19, 212-238.

Talent Irrigation District, District History: Talent Irrigation District. Last accessed on March 24, 2009: <http://www.talentid.org/mn.asp?pg=DistrictHistory>.

U.S. Geological Survey, 2006 (June 9), Upper Klamath Basin ground-water study: Background. Retrieved December 2, 2007, from <http://or.water.usgs.gov/projs_dir/or180/background.html>.

Williams, H., 1942, The geology of Crater Lake National Park, Oregon, Carnegie Institution of Washington Publication 540, 162p.

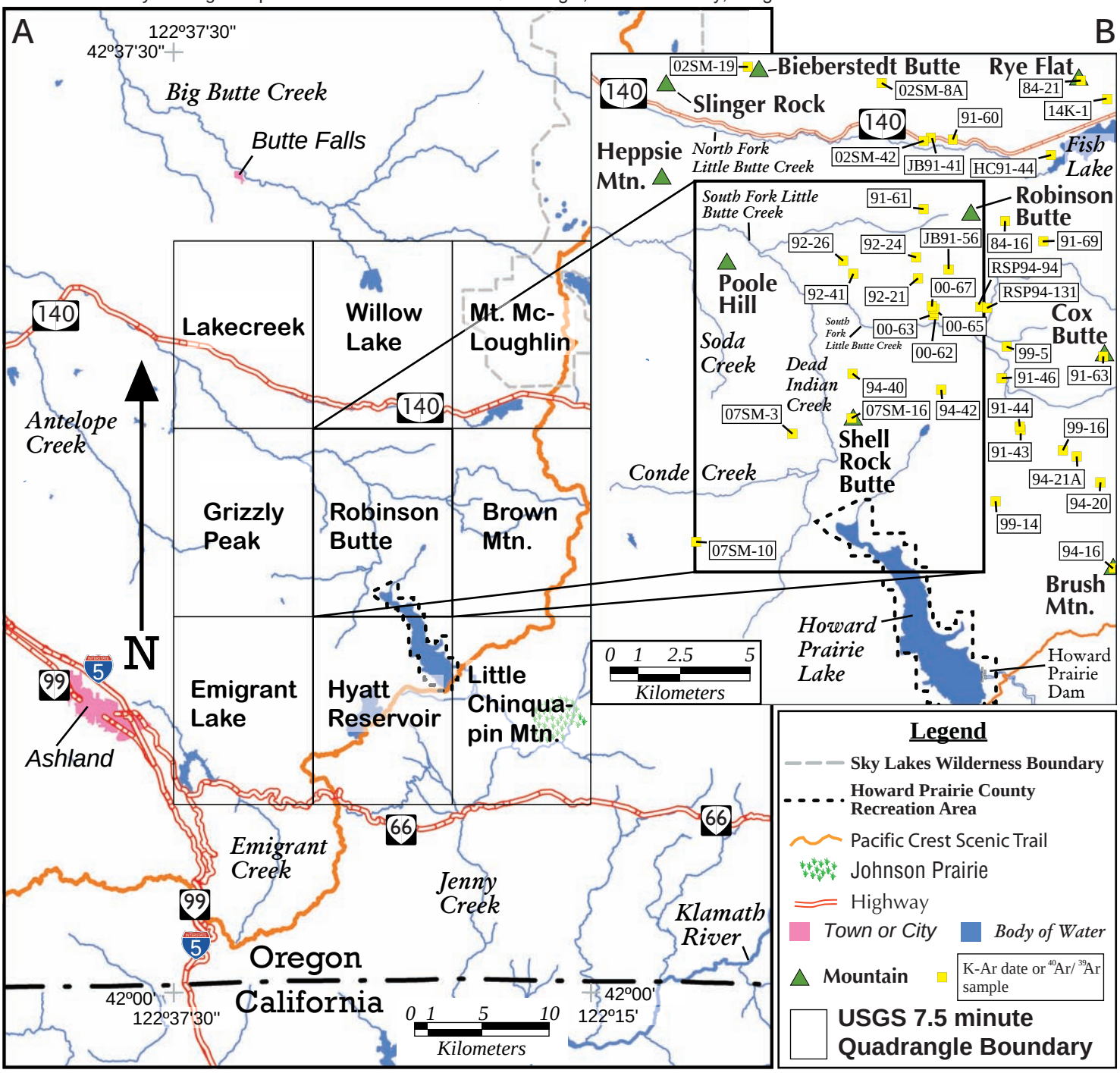

Figure 1. This series of location maps (A through D) provides a broad context in which to place the Preliminary Geologic Map of the Robinson Butte 7.5′ Quadrangle, Jackson County, Oregon. Figures 1C and 1D were modified from U.S. Geological Survey (2006).

Figure 2A. This view is looking from the NE to the SW from the Short Creek drainage across the narrow, steep valley in which the South Fork of the Little Butte Creek flows.

Figure 2B. This image was taken a mile or so further to the west of Figure 2A and is looking from the north to the south across the valley. The stream valley has widened considerably and the valley wall in the far background is the headwall for numerous slumps / landslides that form the hummocky topography in the foreground.

Figure 2C. Moving another mile or so further to the west and looking from the NE to the SW across the South Fork of the Little Butte Creek drainage, the stream has now incised deeply into the Heppsie Formation and the valley walls are much less steep than in both Figures 2A and 2B.

Figure 3A. This currently unused hard rock quarry located in the SW quarter of the Robinson Butte quadrangle provided darker colored basaltic lava as starting material for the aggregate industry. The lavas depicted are part of the Heppsie Formation.

Figure 3B. This hard rock quarry is also currently unused and is located in the west-central part of the quadrangle. The lavas are andesite in bulk composition and are very well jointed, a feature that facilitates their use as a source for road building aggregates. The lavas depicted are part of the Heppsie Formation.

Figure 3C. This photo delineates well-developed flow jointing in an andesite flow of the Heppsie Fomation. One can easily visualize how this material could be more easily broken up into aggregate than more massive less jointed basalt.

Figure 4. Part of the delivery system of canals that carries water from Howard Prairie Lake to the Rogue River drainage further to the west in Jackson County, Oregon.

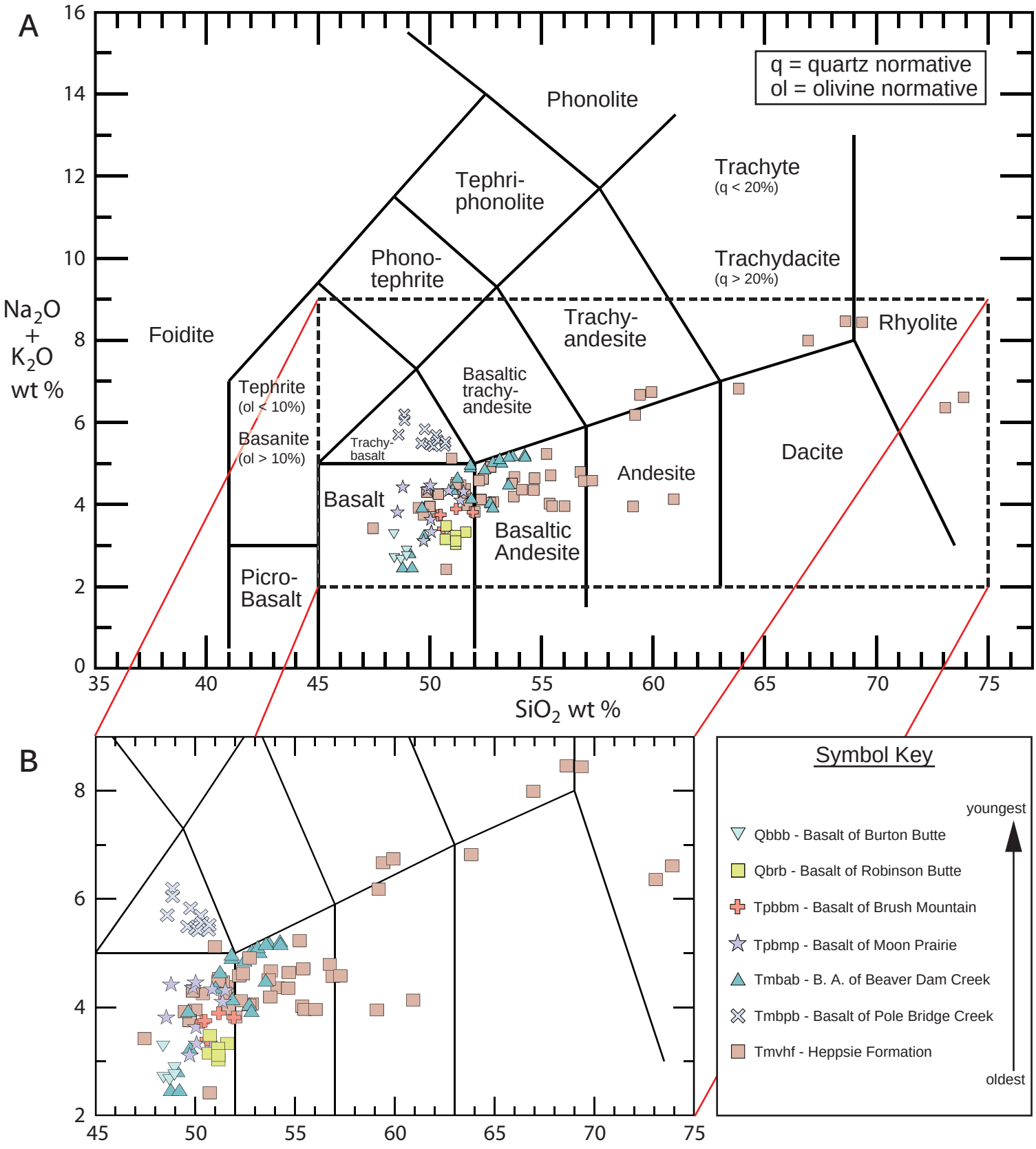

Figure 5. IUGS (International Union of Geological Sciences) classification system for volcanic rocks, which is based on total alkali ($Na_2O + K_2O$) vs. silica (SiO_2) content, with the superimposed data from analyzed Robinson Butte quadrangle samples (except specimens collected on landslides [Qls unit], and including three Tpbbm samples from the southeasterly adjacent Little Chinquapin Mtn. quadrangle, plus two Tpbbm and five Qbbb specimens from the easterly adjacent Brown Mountain quadrangle; see Table 1) (Le Maitre, 2002).

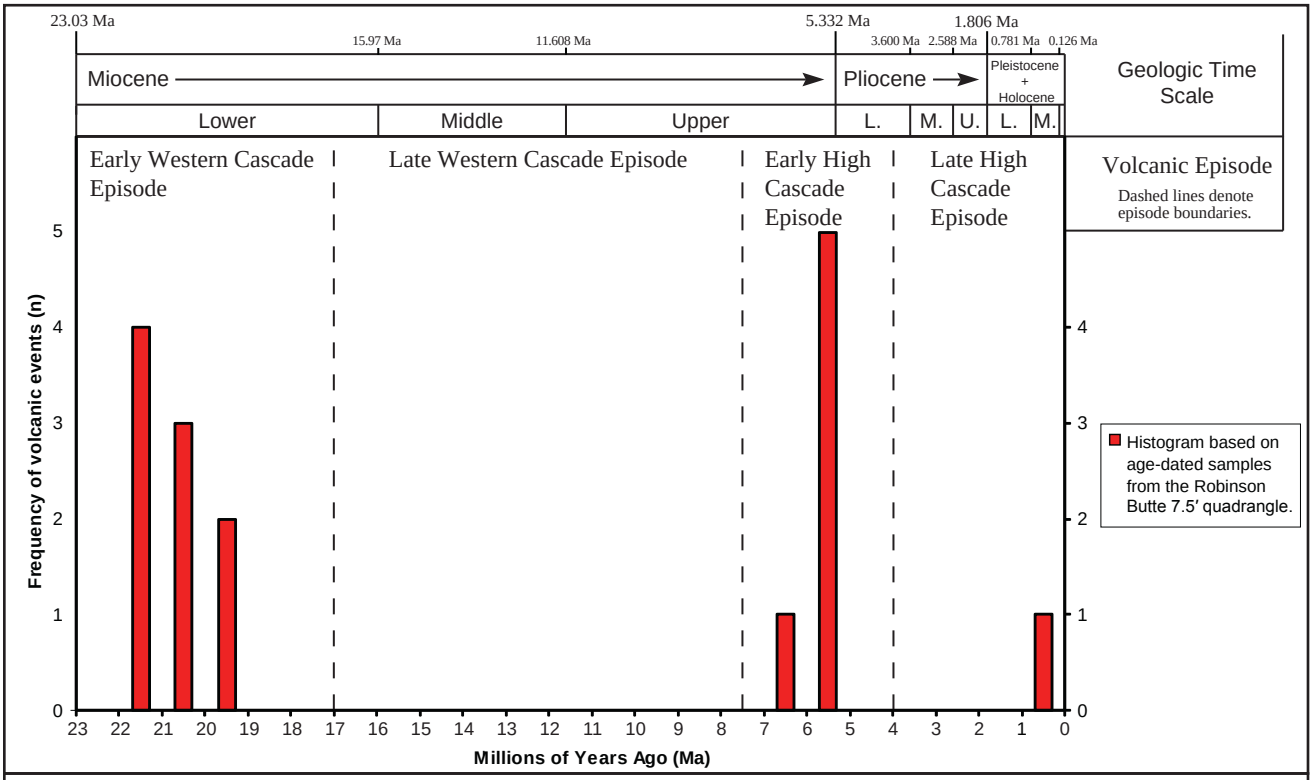

Figure 6A. Histogram (number of samples with either a K-Ar or $^{40}Ar/^{39}Ar$ age date plotted as a function of geologic time in millions of years) of the geochronologic data derived from Robinson Butte quadrangle samples.

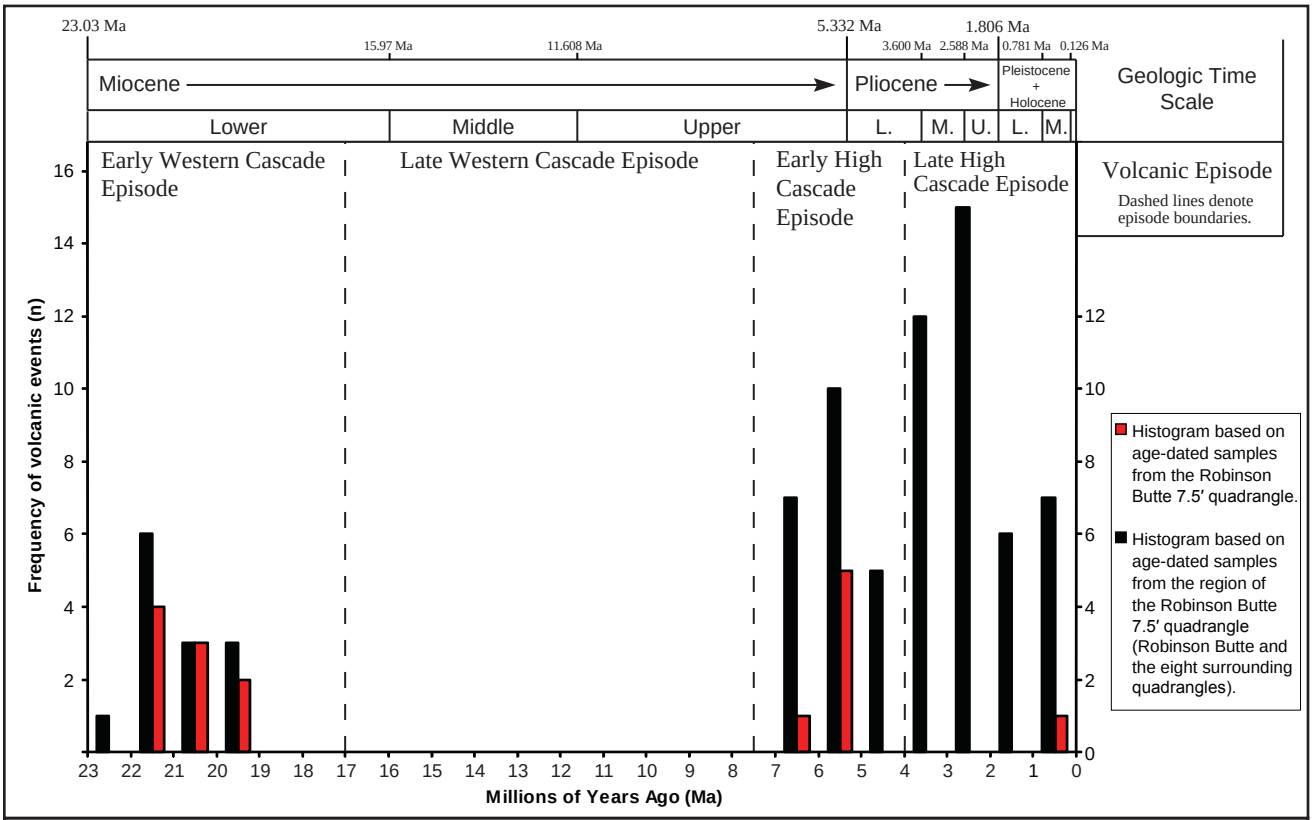

Figure 6B. Histogram of the geochronologic data derived from Robinson Butte quadrangle samples plus the eight surrounding quadrangles (see Figure 1).

Figure 7. On the north side of the South Fork of the Little Butte Creek approximately 3 km west of the Short Creek drainage is the location where this photo of a headwall scarp of a moderately sized landslide / slump was taken. Qls, Quaternary landslide deposits, dominate both sides of the valley as one travels further to the west.

Figure 8. Looking from south to north across the more narrow, canyon-like portion of the South Fork of the Little Butte Creek in the far eastern portion of the Robinson Butte quadrangle, the crude columnar jointing pattern of the more intensely welded portion of the pyroclastic flow(s?) that forms the upper-most portion of the Heppsie Formation is well exposed by erosion.

Figure 9A. Where Short Creek incises down into the upper Heppsie Formation on the north side of the South Fork of the Little Butte Creek in the far eastern portion of the Robinson Butte quadrangle, massive columnar jointing is clearly evident in the lower less intensely welded lighter colored portion of the outcrop which extends upward through approximately half of the darker colored pyroclastic material. A sharp nearly horizontal break cuts the vertically oriented columnar jointing pattern and coupled with some $^{40}Ar/^{39}Ar$ dates from the adjacent to the north Willow Lake quadrangle (see Figure 1) combine to suggest the existence of at least two pyroclastic flows rather than one chemically zoned flow.

Figure 9B. This photo depicts the heterolithologic make-up of the material that constitutes the non to weakly welded section of the upper portion of the Heppsie Formation. Foreign rock fragments and pumice pieces are held together by finer lapilli and ash sized material.

Figure 10. Easily worked by road grading equipment, slopes of poorly welded Heppsie Formation pyroclastic flow material constitute a number of outcrops along the north side of Oregon Route 140 traveling west of Fish Lake and beyond the turn-off to Butte Falls.

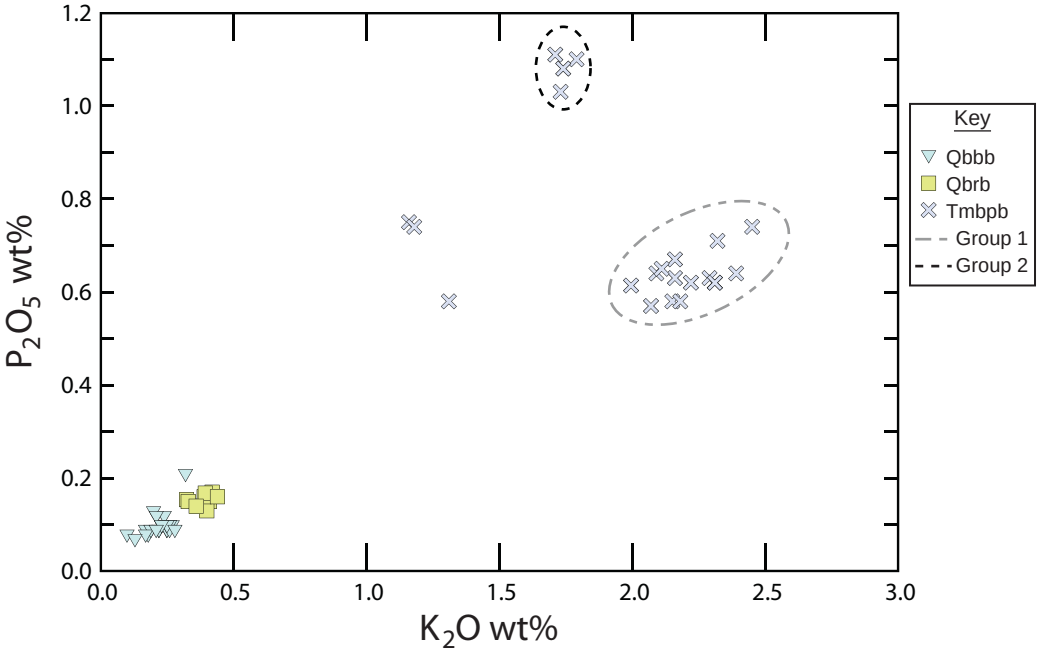

Figure 11A. To emphasize the distinctiveness of the Tmbpb lavas, chemical data was plotted on a P_2O_5 versus K_2O variation diagram for it, Qbbb, and Qbrb. The data points for the latter two units plot relatively near the origin, a chemical characteristic of many of the basaltic units associated with the Cascade volcanic province (Hughes, 1990; Leeman and Others, 1990). However, the Basalt of Pole Bridge is quite atypical and can be easily separated into two groups based on petrographic and chemical criteria (see text and Figures 22-26).

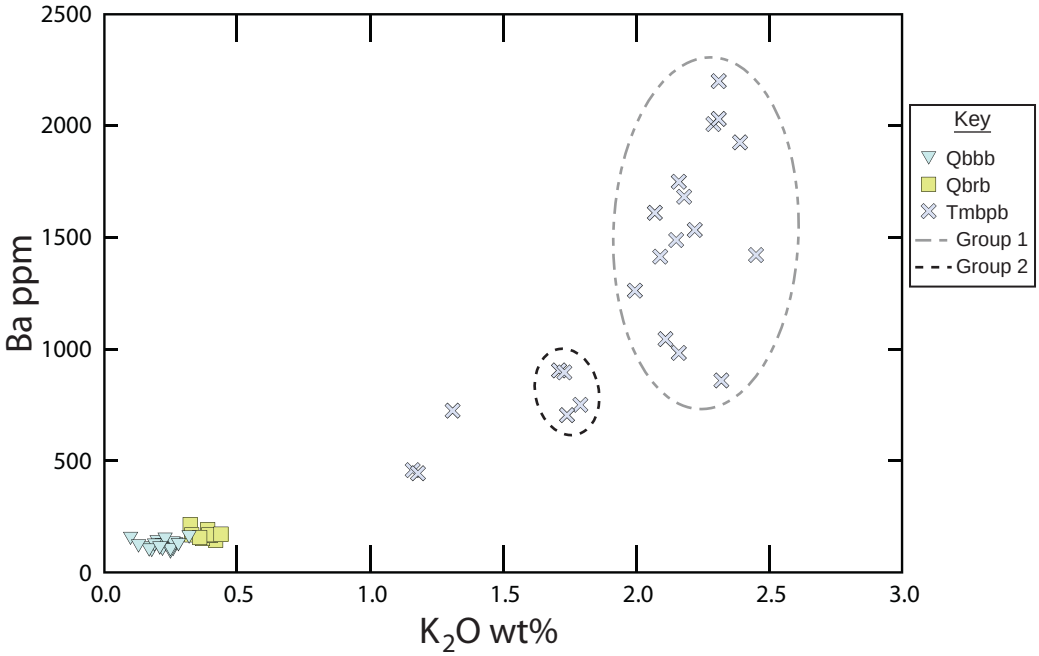

Figure 11B. The chemical distinctiveness of Basalt of Pole Bridge samples is well exhibited by the Ba versus K_2O diagram. Given the high MgO concentration in Tmbpb lavas there is little evidence suggestive of extensive differentiation. Therefore, it is likely the elevated Ba contents reflect the source of the Tmbpb magma. What mantle phase contributed the Ba to the primary Tmbpb magma? Presently, there is no answer to this question.

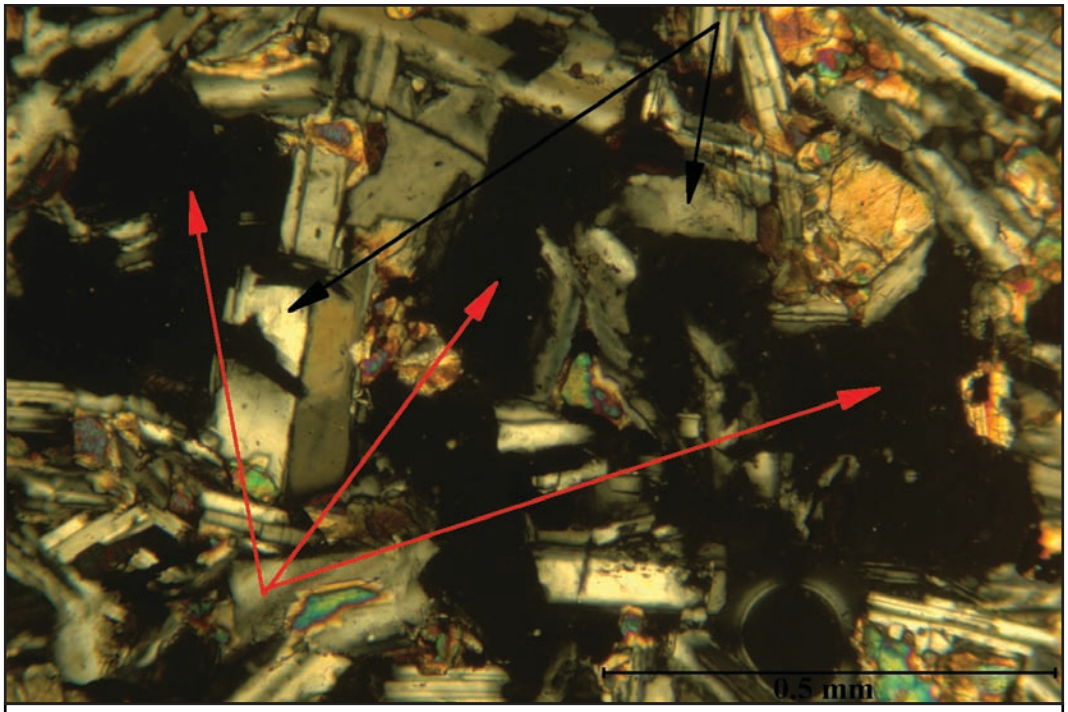

Figure 12. This photomicrograph of Burton Butte lava was taken with the polarizing filters crossed, thus producing the optical property known as birefringence where minerals such as plagioclase are colored and isotropic substances like glass are black. The red arrows are pointing out black voids that are irregularly shaped gas cavities known as vesicles. In this type of lower silica basalt the vesicles are often intimately intertwined with the matrix forming minerals forming what is termed a diktytaxitic texture.

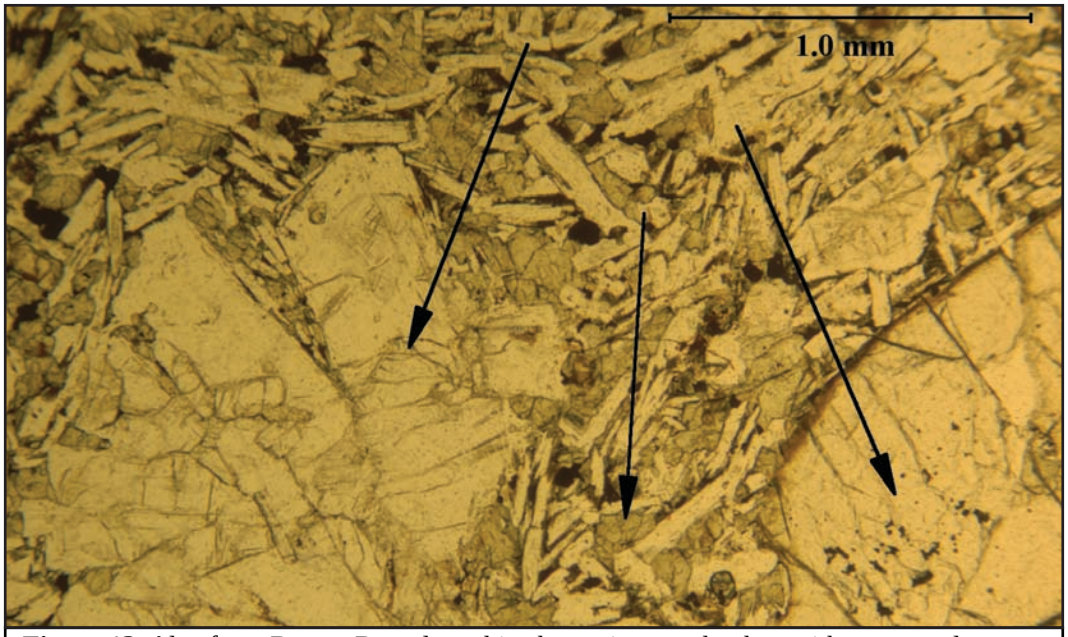

Figure 13. Also from Burton Butte lava this photomicrograph taken with uncrossed polarizing filters, depicts a singular large olivine phenocryst that contains small opaque crystals of chromite to magnetite and has a thin margin of brownish low temperature alteration known as iddingsite (see right hand arrow). The left hand arrow is pointing out a glomeroporphyritic clump of olivine and plagioclase feldspar crystals, suggesting that both of these minerals precipitated out of magma simultaneously for some length of time. The middle arrow is delineating a clinopyroxene crystal that has molded itself around the margins of an earlier formed plagioclase crystal, thus forming what is known as a subophitic texture.

Figure 14A. This panorama was photographed from the extreme south central margin of the Robinson Butte quadrangle looking to the north-northeast and captures Robinson Butte on the left side and Mount McLoughlin on the right side.

Figure 14B. This panorama was photographed from near the boat launch facility on the north side of Fish Lake looking toward the west end of the lake. Robinson Butte is ellipsoidal in shape and is broadly stretched out in a north-south orientation. It is likely the result of what started out as a fissure eruption that subsequently became more of a point source eruption that produced much pyroclastic material (bombs, lapilli, to ash-sized material) in the form of a scoria ridge to cone structure.

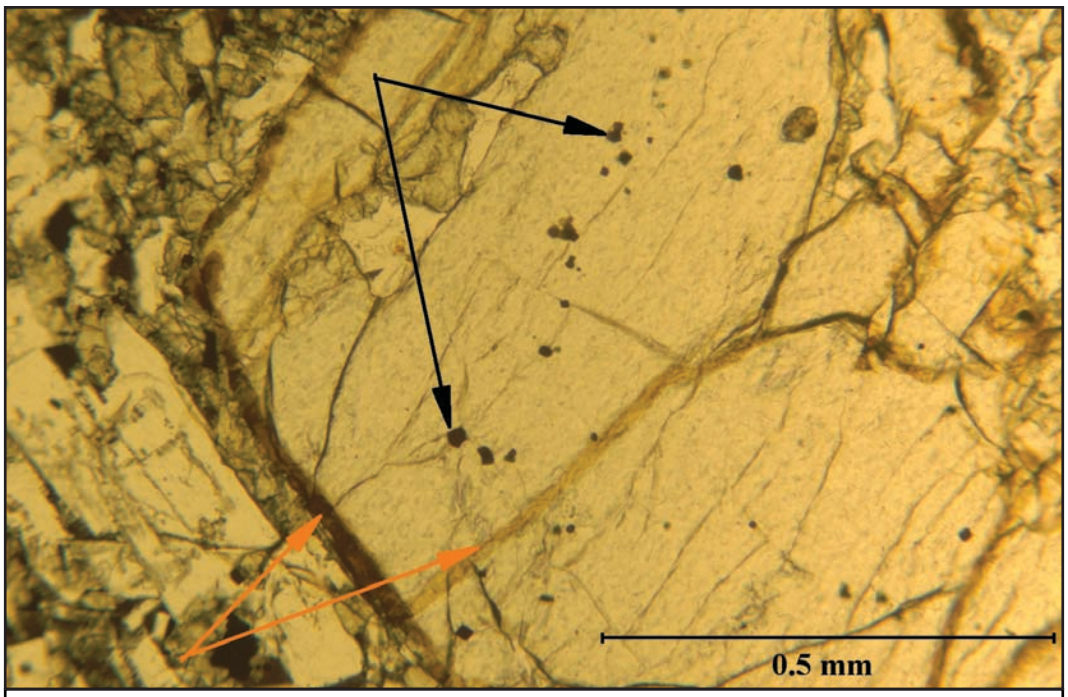

Figure 15. This photomicrograph of a large olivine phenocryst from Robinson Butte lava, taken in plane-polarized light, has two important features: the black arrows point to early formed opaque crystals that likely range from chromite to magnetite in composition and the orange arrows point to iddingsite alteration that has formed on the margin of the phenocryst and permeated along the fracture passing into the interior of the crystal.

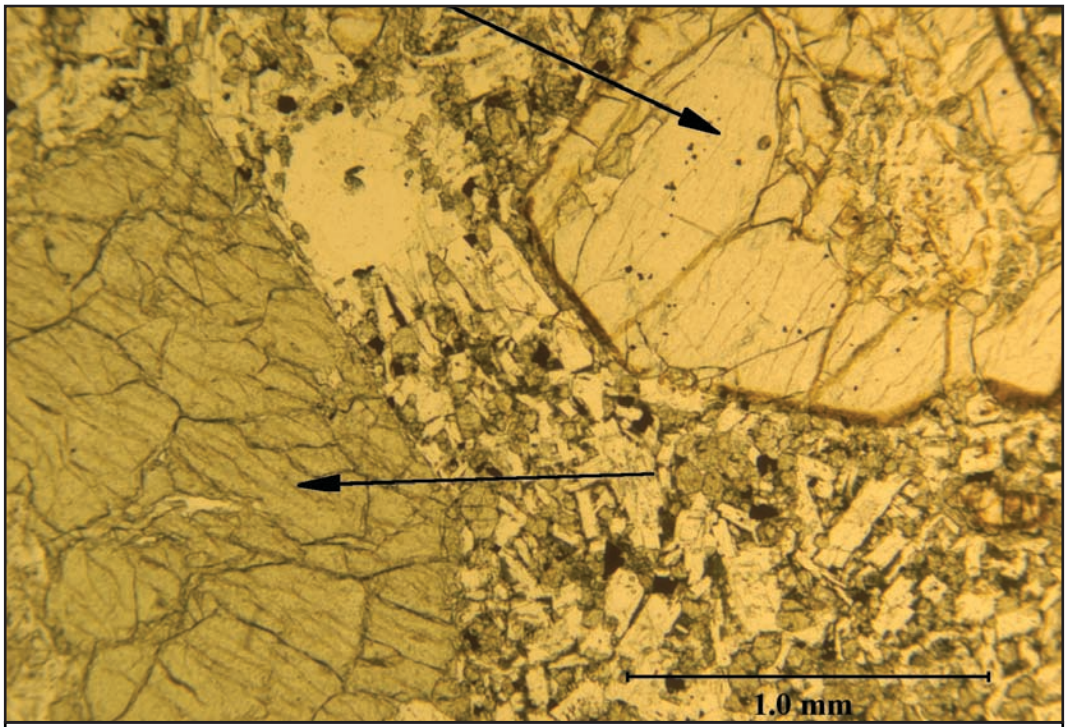

Figure 16. One of the distinguishing characteristics of Robinson Butte extrusive material is the presence of both olivine (top arrow) and clinopyroxene (bottom arrow) as large (2 to 3 mm in diameter) phenocrysts that are depicted in this photomicrograph taken in plane polarized light. Please note the thin margin of iddingsite on the perimeter of the olivine; note the lack of it on the clinopyroxene crystal.

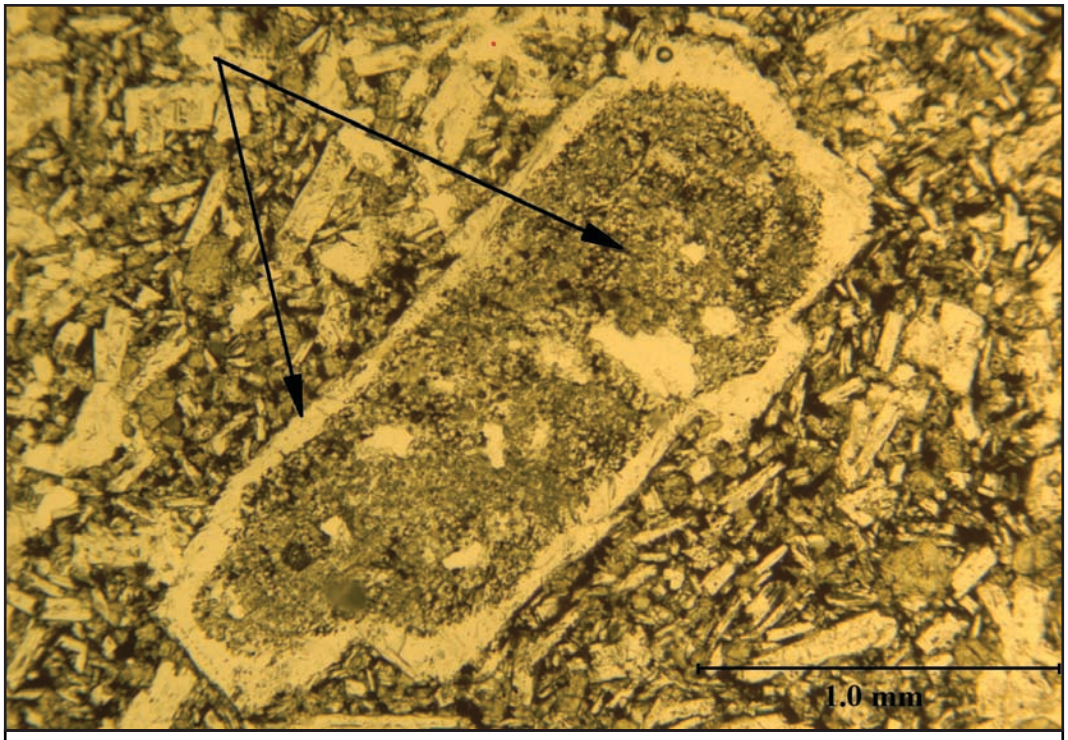

Figure 17. A second distinguishing characteristic of Robinson Butte extrusive material is the presence of half dozen or so plagioclase feldspar phenocrysts, 1 to 2 mm in diameter, per hand sample or thin section that do not resemble the majority population of plagioclase crystals. This photomicrograph taken in plane polarized light depicts a severely corroded and resorbed plagioclase crystal that has had a clear stable margin precipitated around what is now the corroded interior.

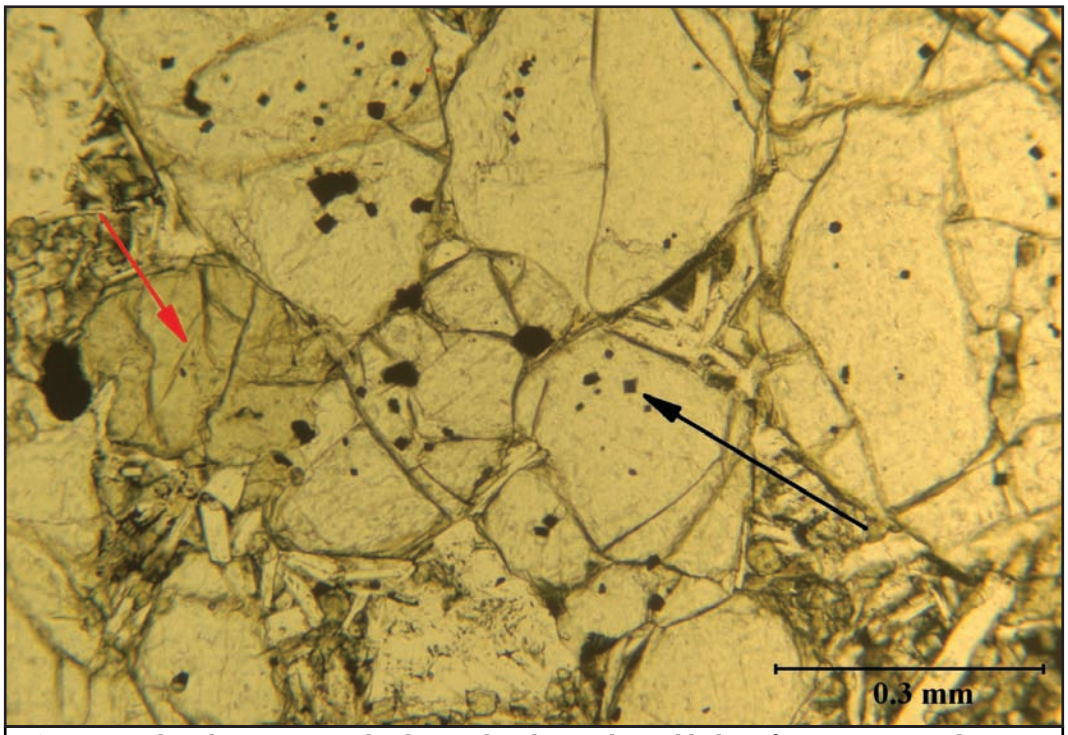

Figure 18. This photomicrograph taken under plane polarized light is from more coarsely crystalline Basalt of Moon Prairie (Tpbmp) lava. The black arrow on the left is pointing out the poikilitic opaque chromite to magnetite grains in olivine while the black arrow to the right is indicating greenish serpentine, a hydrous layered secondary silicate alteration mineral formed under low temperature conditions. Serpentine often forms veins that permeate primary olivine crystals (Neese, 2004). The red arrow is indicating a clinopyroxene crystal that lacks both the opaque inclusions and the serpentine alteration.

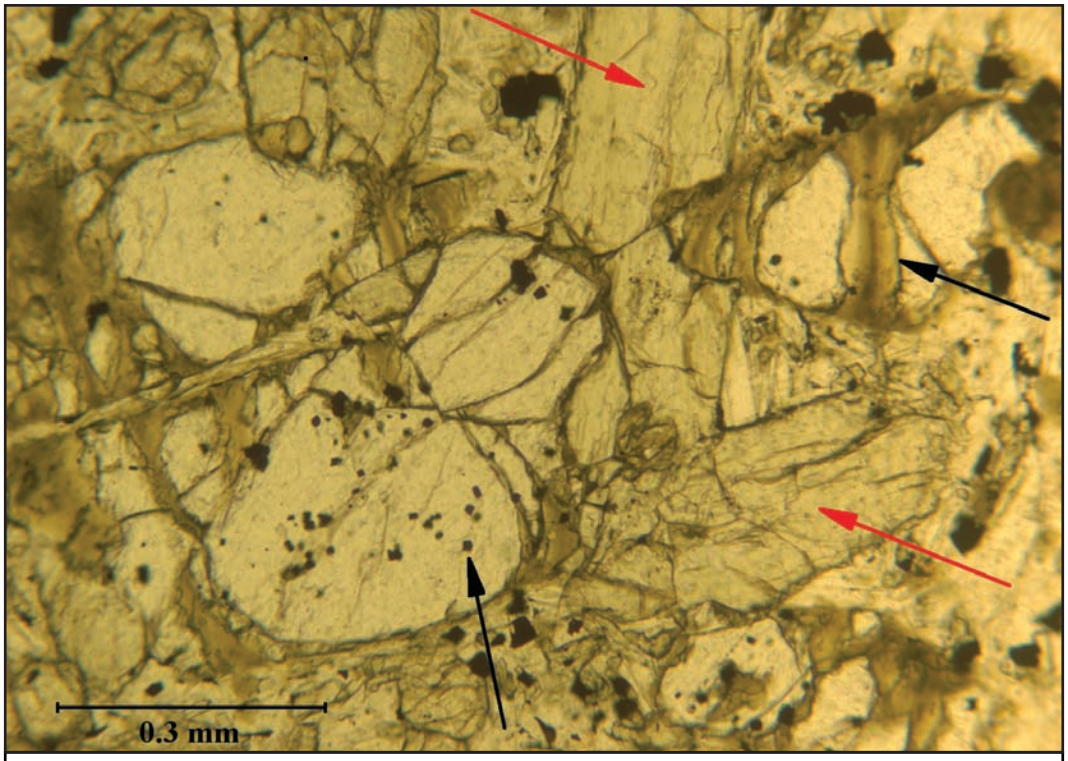

Figure 19. This photomicrograph taken under plane polarized light is from more coarsely crystalline Basalt of Moon Prairie lava. The black arrow on the left is pointing out the poikilitic opaque chromite to magnetite grains in olivine while the black arrow to the right is indicating greenish serpentine, a hydrous layered secondary silicate alteration mineral formed under low temperature conditions, forming veins that permeate primary olivine crystals (Neese, 2004). Two red arrows are indicating clinopyroxene crystals that lack both the opaque inclusions and the serpentine alteration.

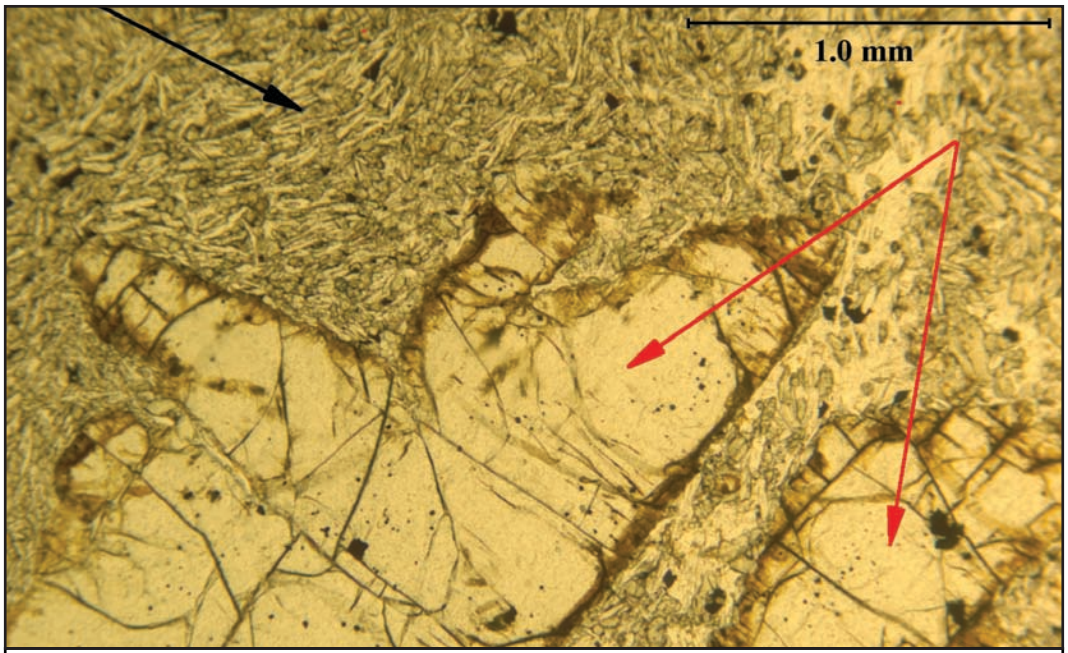

Figure 20. The most frequently encountered Basalt of Moon Prairie lava is one in which olivine phenocrysts (see red arrows), often with iddingsite rims, are established in a fine grained flow aligned matrix of much smaller crystals, forming a trachytic texture. This photomicrograph taken under plane polarized light depicts such a texture in which plagioclase and pyroxene constitute the sea of small grains in which the olivine phenocrysts reside.

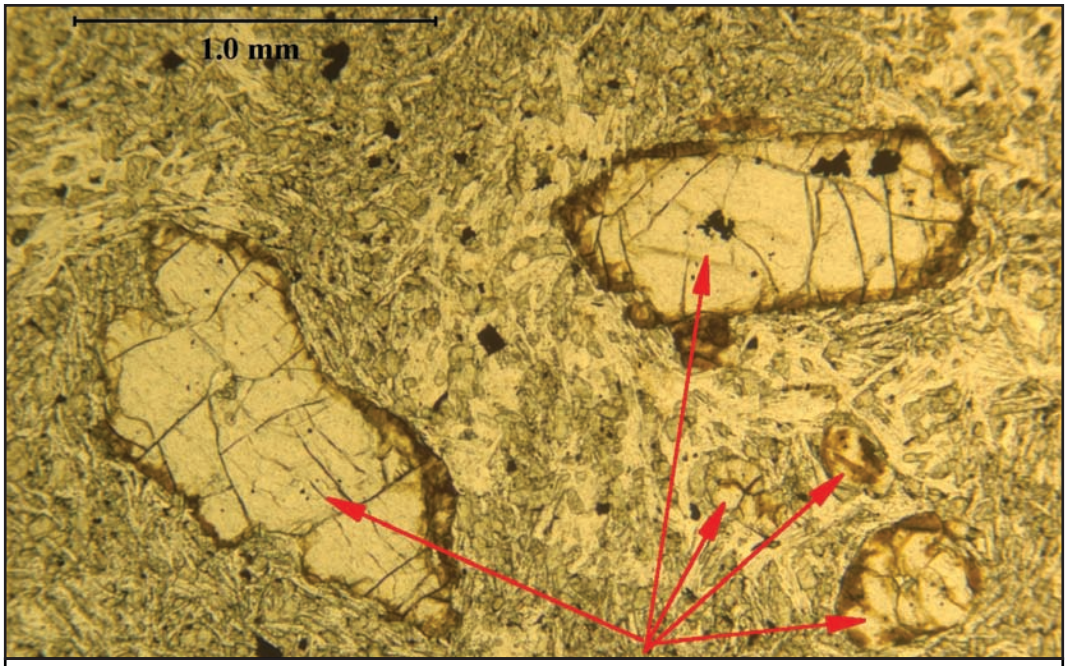

Figure 21. All five arrows are pointing to olivine crystals of various sizes; each crystal has been partially altered to iddingsite. This photomicrograph taken under plane polarized light provides a good example of what is termed “olivine-phyric basalt”; that is, basalt with phenocrysts of only olivine with all the additional minerals being confined to the matrix of the sample. The thin section texture depicted is best termed intergranular. The lava sample is from Tmbab Basaltic Andesite of Beaver Dam Creek.

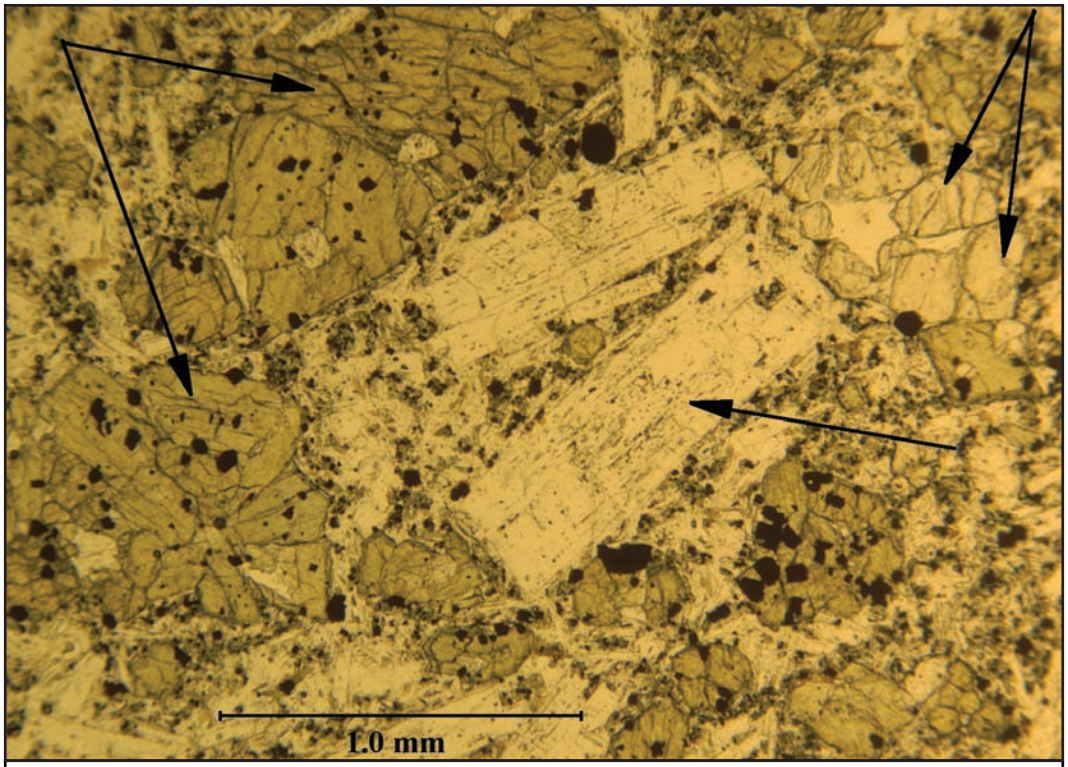

Figure 22. This photomicrograph of Basalt of Pole Bridge Creek (Tmbpb) group 1 lava taken under plane-polarized light shows a glomeroporphyritic clump of clinopyroxene phenocrysts (two black arrows on left hand side) that are quite poikilitic with opaque magnetite crystals. Also depicted are plagioclase phenocrysts in euhedral rectangular-shaped (laths) (see middle arrow) and small, unaltered olivine phenocrysts (see two arrows on right hand side of image). The sheer amount of opaque mineral present and their relatively large sizes are noteworthy.

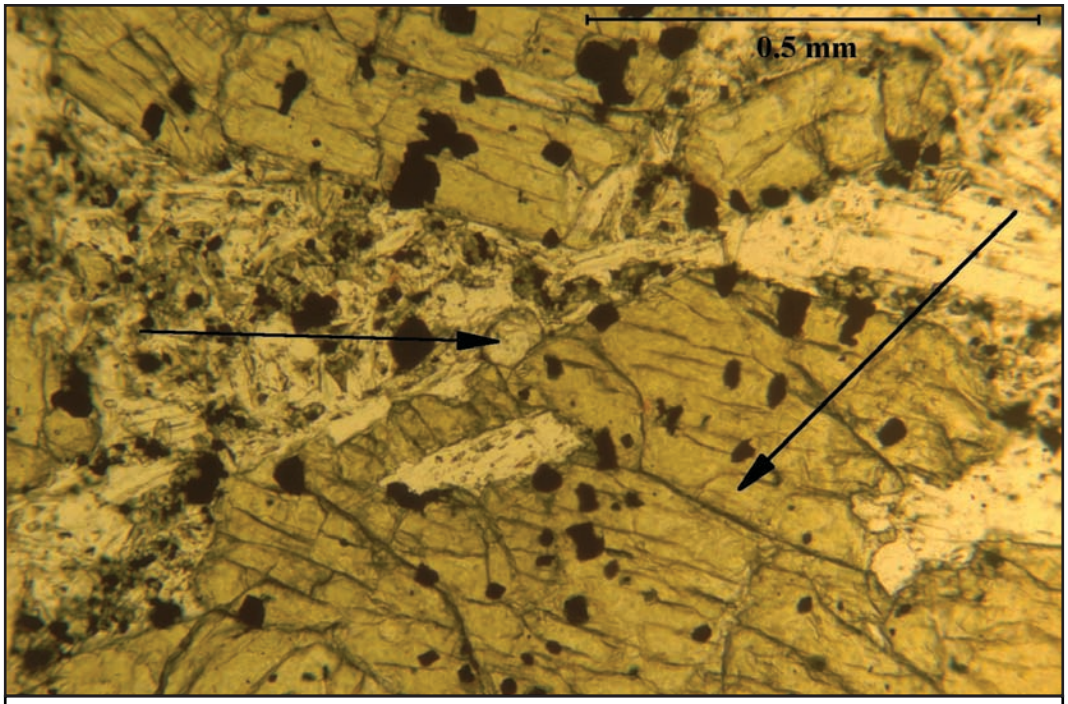

Figure 23A. This photomicrograph is a close-up of Tmbpb lava with its characteristic glomeroporphyritic clumps of clinopyroxene, with individual crystals quite poikilitic with opaque magnetite grains (see arrow on the right). Olivine (see arrow on the left) is much less abundant than clinopyroxene, an unusual occurrence in the basaltic rocks of the Cascade Mountains of south-central Oregon.

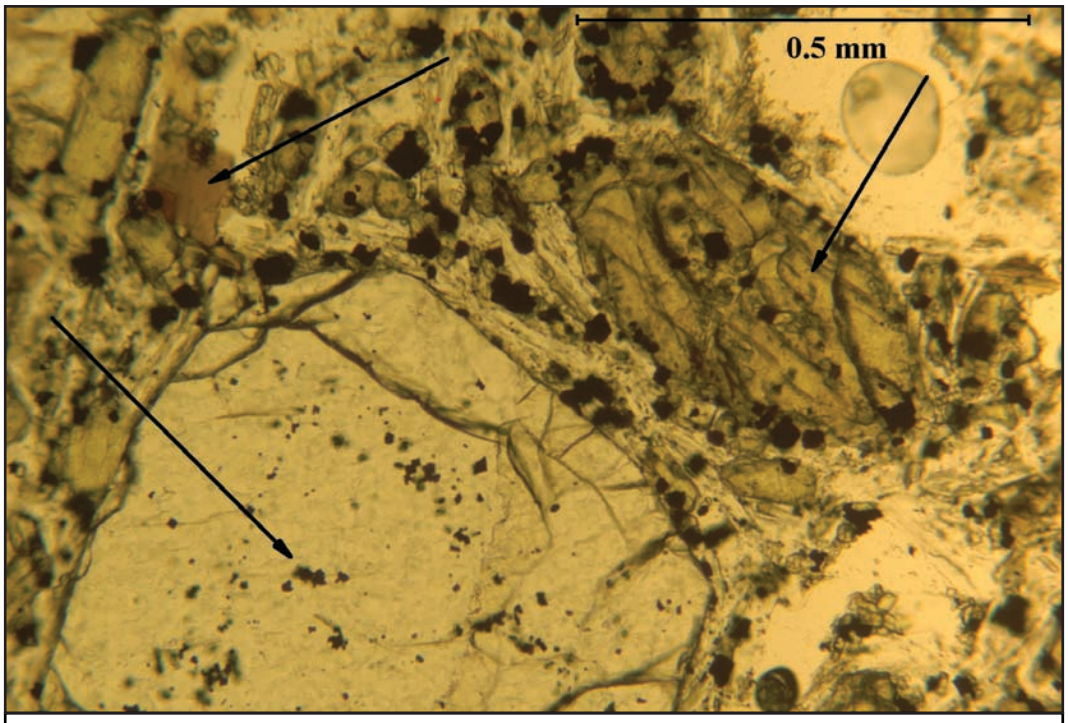

Figure 23B. The lower left arrow in this photomicrograph delineates an olivine phenocryst quite rich with opaque chromite to magnetite inclusions while the arrow on the right is indicating a smaller phenocryst of clinopyroxene. The arrow toward the upper left corner marks a mineral that is found only in the high K_2O trachybasalt lava of Tmbpb. The mineral is an iron-rich biotite that is pleochroic in brown, is consistently less than 0.1 mm in diameter, and crystallizes very late in the solidification history of these lavas. It may be the result of vapor-phase crystallization.

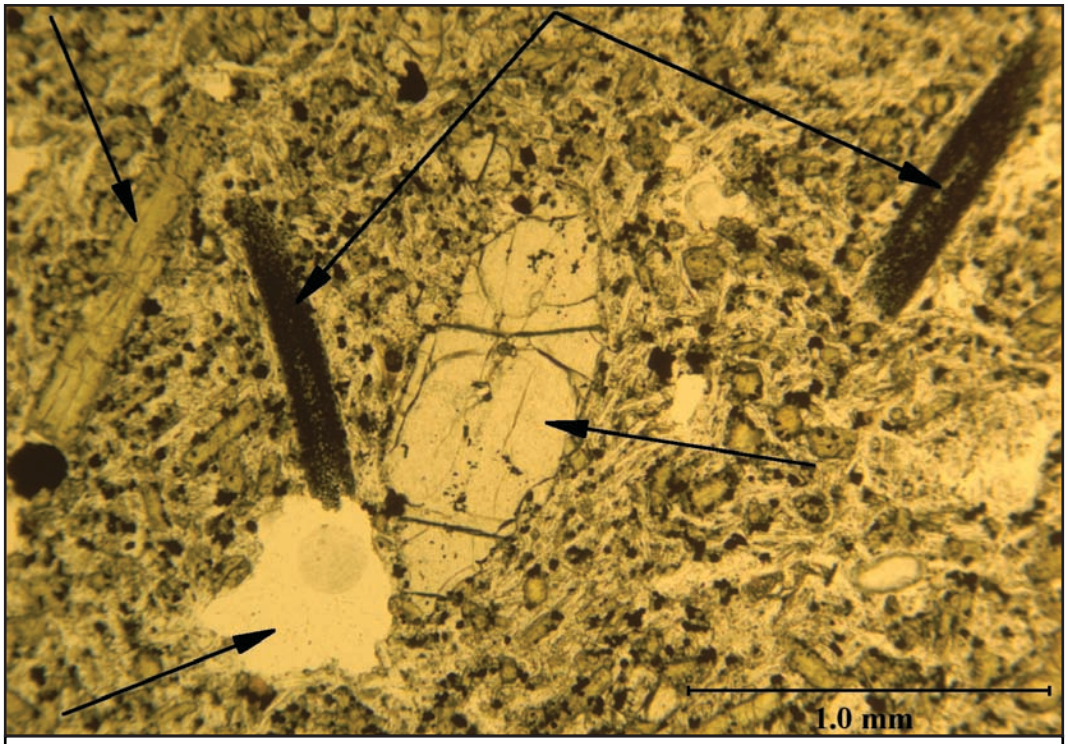

Figure 24. The arrow to the lower left in this photomicrograph taken under plane-polarized light of Group 2 (see Figures 11A and B) Tmbpb lava, is pointing out an irregularly shaped large vesicle. Working sequentially from left to right the singular arrow delineated a long but thin phenocryst of clinopyroxene while the double arrow radiating from a singular point mark two pseudomorphs that have replaced the original mineral that had initially crystallized. This phenomenon is a unique characteristic of Group 2 Tmbpb lava. A euhedral olivine phenocryst occupies the center of the photomicrograph and shows no sign of alteration.

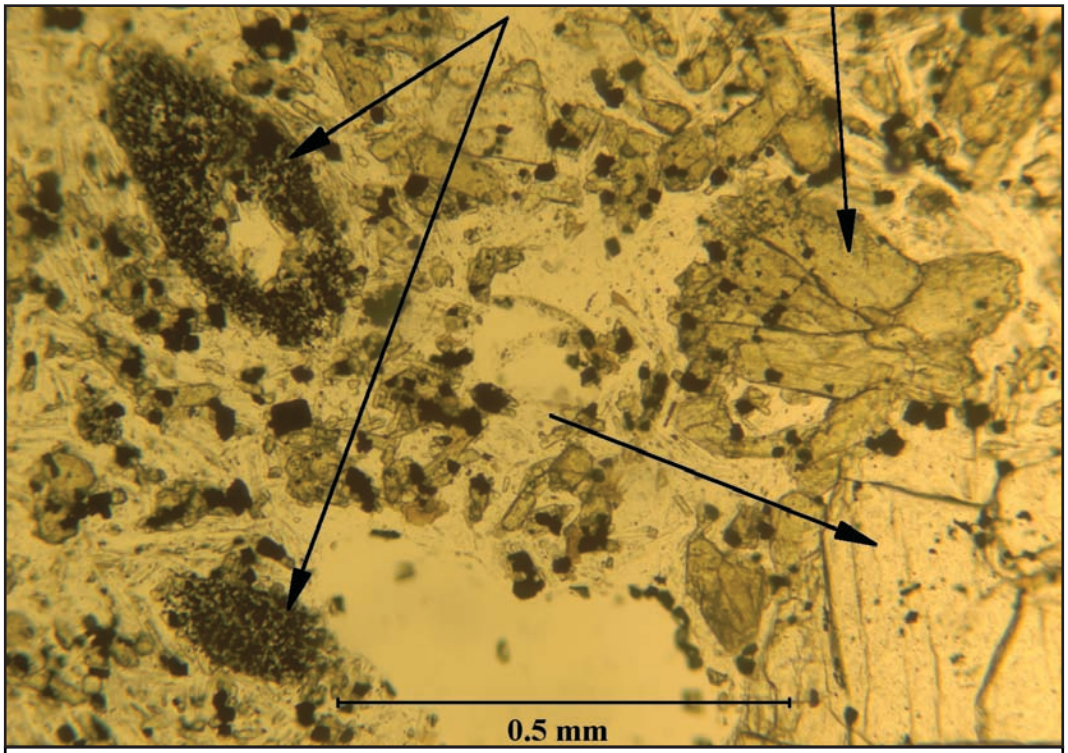

Figure 25. The pseudomorphs, in particular the one to the upper left portion of the photomicrograph, by their external shape can provide a clue to the nature of the original primary mineral to crystallize. The six-sided nature of the upper left form, together with the blunt terminations, is quite suggestive an amphibole, mostly likely a member of the hornblende family of hydrous minerals. To the right the upper arrow points to a clump of clinopyroxene phenocrysts; to the lower right is olivine with its ubiquitous inclusions of opaque chromite to magnetite grains.

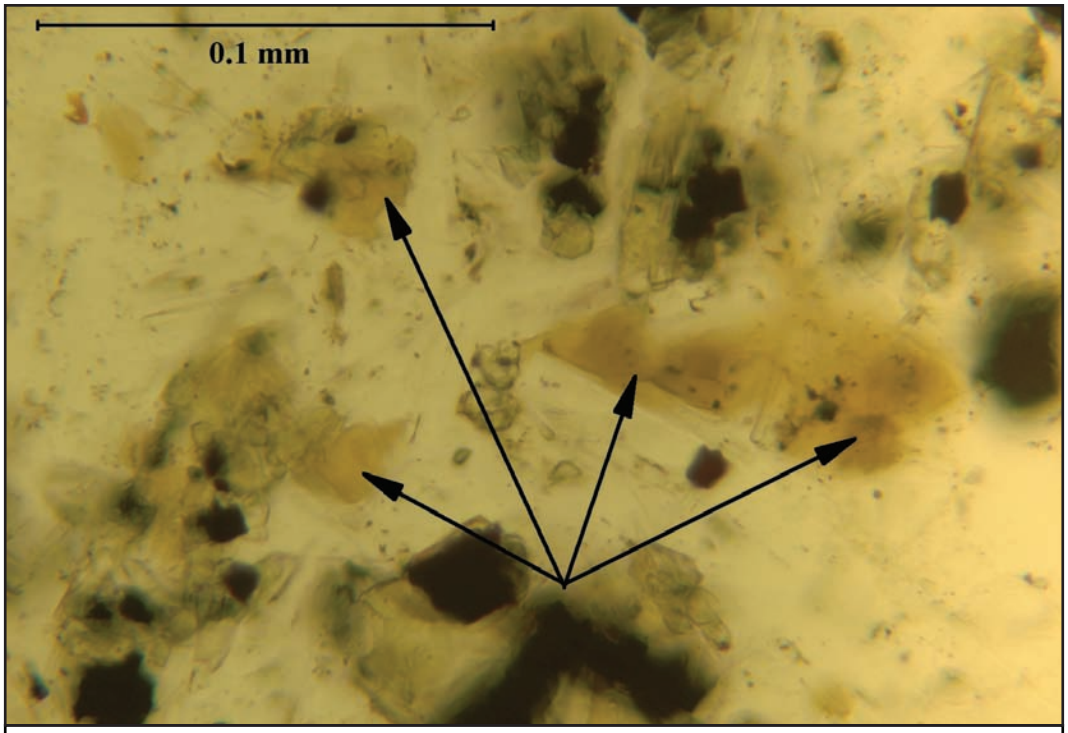

Figure 26. In this highly magnified photomicrograph of Group 2 Tmbpb lava the four arrows indicate scattered discrete anhedral crystals of iron-rich biotite. The high K_2O content coupled with the availability of iron and water vapor (fluorine may or may not be an important factor, too) set the stage for the crystallization of this unusual groundmass-forming mineral.

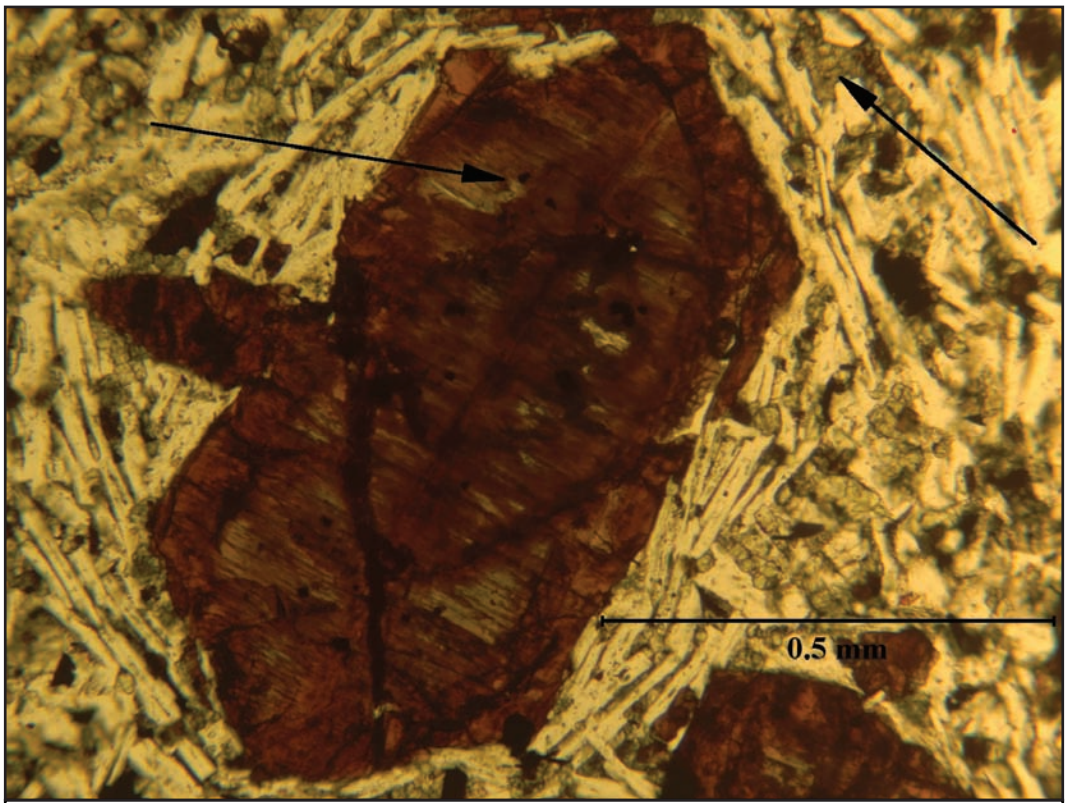

Figure 27. This photomicrograph depicts the common state of olivine phenocrysts in basaltic lava flows of the Heppsie Formation; that is, completely altered under low temperature conditions to the mineral assemblage known as iddingsite (Baker and Haggerty, 1976; Neese, 2004). Notice the euhedral shape of the original olivine crystal has been preserved during the alteration process, thus forming a pseudomorph.

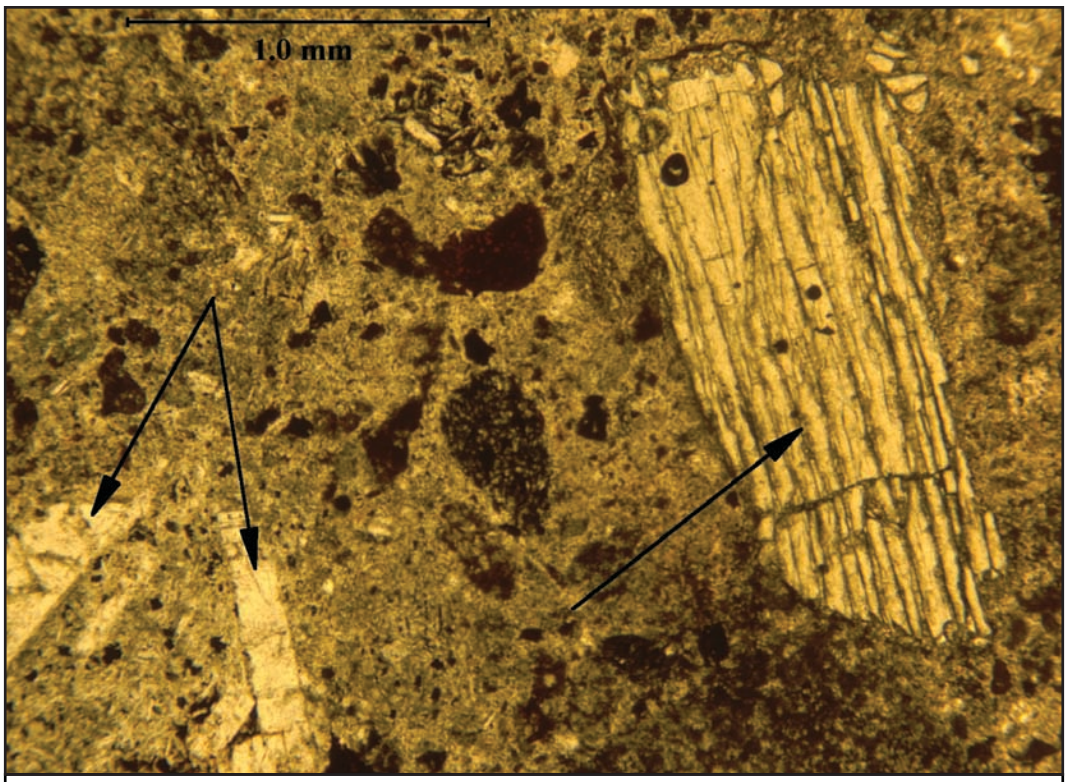

Figure 28. While olivine has suffered considerable alteration within the Heppsie Formation, this photomicrograph depicts the normal state of affairs for clinopyroxene (arrow to the right) and plagioclase (two arrows on the left). The clinopyroxene is pristine; it shows no sign of post-crystallization alteration. The plagioclase crystals are sometimes fractured with some secondary minerals present in the cracks but for the most part the plagioclase is intact.

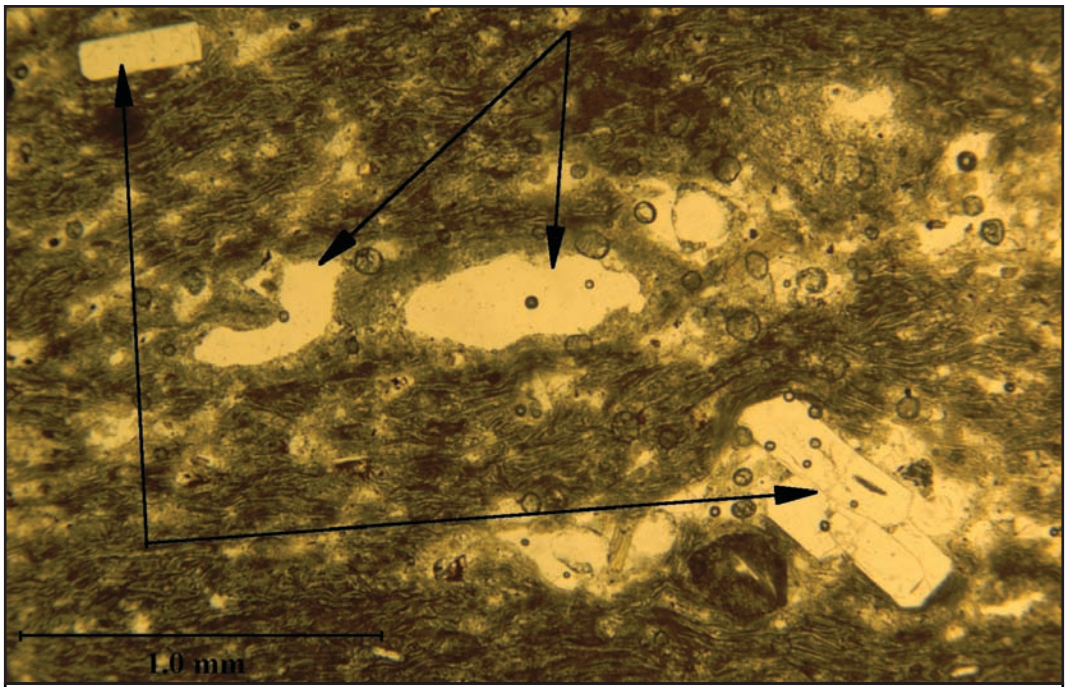

Figure 29. The following set of six photomicrographs (Figures 29 through 34) is from the Short Creek stratigraphic section through the pyroclastic flow members of the upper-most portion of the Heppsie Formation. This first photomicrograph taken under plane-polarized light details the sparse number of phenocrysts typically present in the lower, less intensely welded pyroclastic flow. Two plagioclase feldspar phenocrysts (upper left and lower right) and two vesicles, centrally located, are noteworthy.

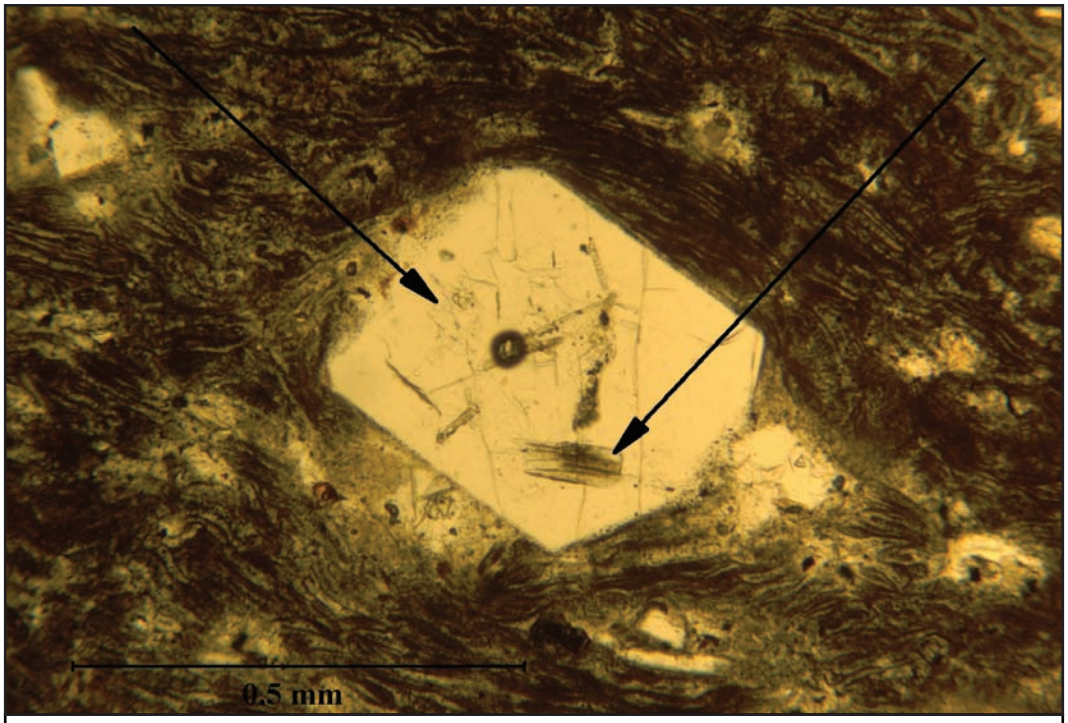

Figure 30. Within the phenocrysts of plagioclase feldspar (left hand arrow) as depicted in this photomicrograph are often mineral inclusions of earlier crystallized minerals, in this case, apatite (right hand arrow).

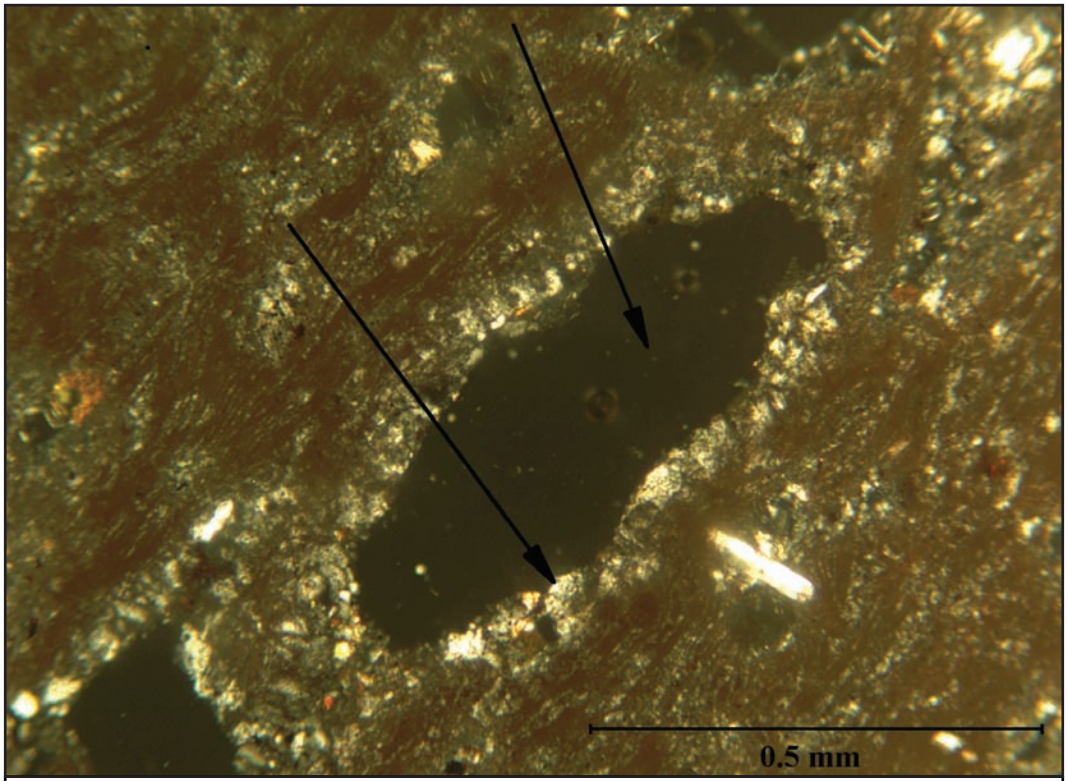

Figure 31. Around the exterior walls of many of the vesicles (see lower left arrow) within pyroclastic flows, evidence for vapor phase crystallization will often be encountered. This photomicrograph, taken under crossed polarizers to better see the birefringent mineral grains that line the vesicle walls, depict quite small quartz and feldspar crystals that likely formed after the crystallization event for the pyroclastic flow was complete. The vesicles themselves (upper right arrow) are often stretched out in the direction of flow and squashed by the weight of the overlying fragmental material.

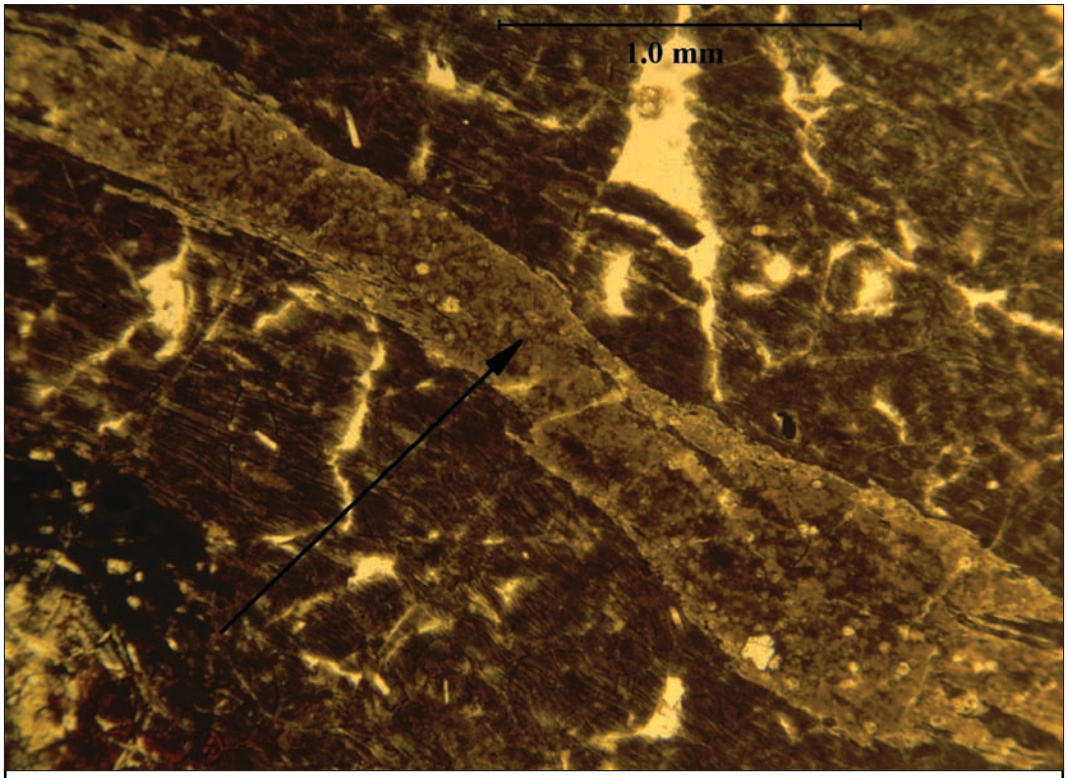

Figure 32. This photomicrograph is from the upper of the two pyroclastic flows that outcrop in the Short Creek drainage, the one that is more siliceous and more intensely welded. Depicted in this image taken in plane-polarized light is a flattened lump of pumice that owes its shape to a combination of higher temperature and the weight of the overlying pyroclastic flow material.

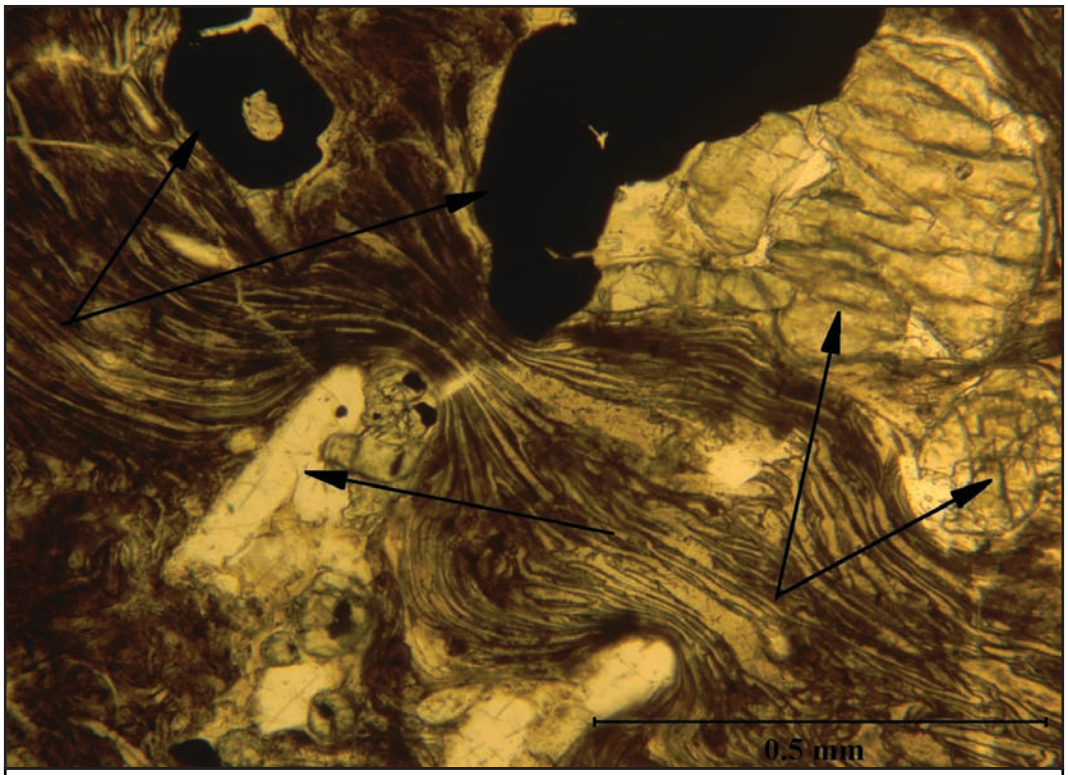

Figure 33. Lines of flowage are vividly depicted in this photomicrograph taken in plane-polarized light. Swirling about the early-formed phenocrysts of clinopyroxene (two arrows on the right), plagioclase feldspar in the center, and an opaque mineral, most likely magnetite (two arrows to the left), the glassy to cryptocrystalline matrix clearly portrays the intensity of the extrusive event that formed this pyroclastic flow.

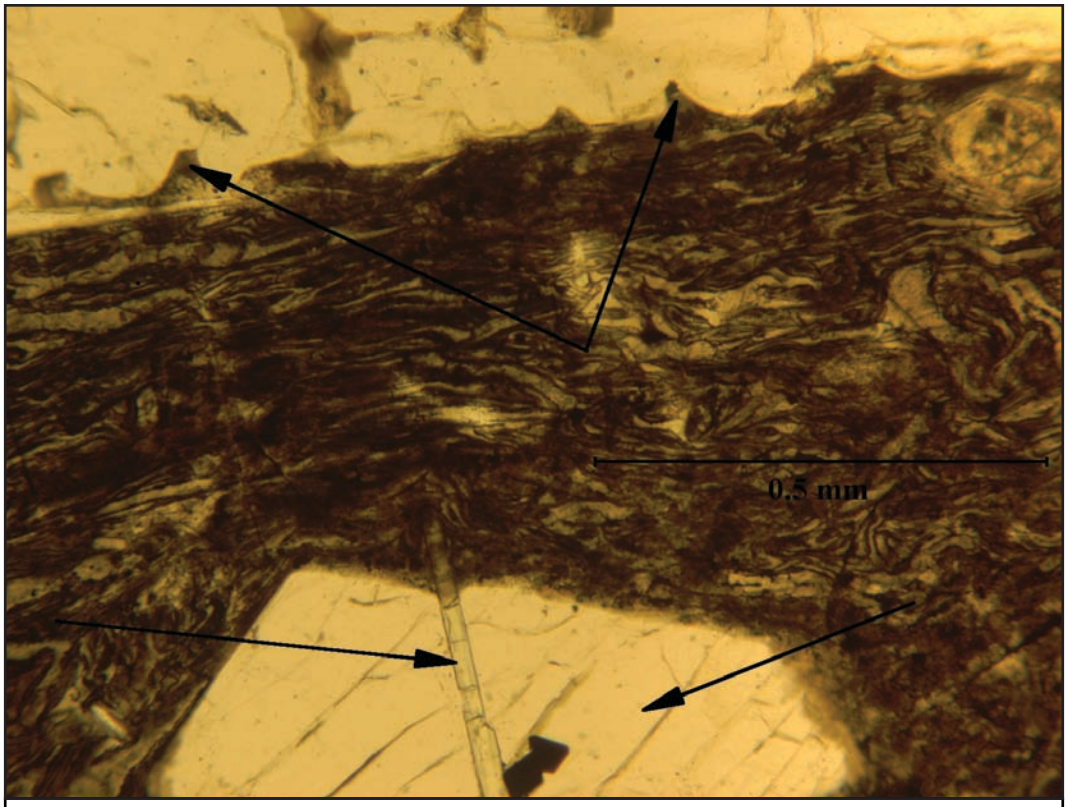

Figure 34. This photomicrograph taken under plane-polarized light conveys two messages. In the lower half of the image plagioclase feldspar (right arrow) has grown around an earlier formed long thin euhedral apatite crystal (left arrow) and two opaque mineral grains. Observations such as this one provides a clue concerning the sequence in which the minerals have crystallized. In the upper portion of the image is the external margin of a large plagioclase phenocryst. Note the indented nature of that margin (see the two upper arrows) that forms what is termed a cuspate interface. It looks something like a seriate edge of knife blade. This texture likely resulted from the decompression of the magma as it moved to the surface, an event that often leads to a temperature increase. Naturally the plagioclase crystal is no longer in thermal equilibrium with its surroundings, so it begins to react, thus producing the texture depicted above.

Table 1 (page 1). Whole rock chemical data and potassium-argon (K-Ar) ages ([a] indicates an argon-argon age) for the samples from the Preliminary Geologic Map of the Robinson Butte 7.5′ Quadrangle, Jackson County, Oregon. The major element oxides are presented in weight percent and the trace elements are reported in parts per million (ppm). The chemical data are X-ray fluorescence (XRF) results and were measured in the X-ray laboratory of the Department of Earth and Environment, Franklin and Marshall College, Lancaster, Pennsylvania. The UTM coordinate values are according to the UTM Zone 10 (NAD 27 for US) projection. All UTM coordinates have been rounded to the nearest 10 m. The 1/4 of 1/4, 1/4, Section (Sec.), Township (T.), and Range (R.) columns are location descriptors of the Public Land Survey System (PLSS: Willamette meridian and base line). In the Lithology column (Lith.), B = basalt (SiO_2 = 45-52%), BA = basaltic andesite (SiO_2 = 52-57%), A = andesite (SiO_2 = 57-63%), D = dacite (SiO_2 = 63-74%), Rhy = rhyolite, TrB = trachybasalt, TrA = trachyandesite, and Tr = trachyte (consult Figure 5 of this report). See Figure 5 and Le Maitre (2002) for details regarding lithological classification. Please consult the detailed descriptions in this report or the geologic map for the full unit names. This table is 3 pages long.

Map no.	Sample no.	K-Ar Age([a]) Ma	1/4 of 1/4	1/4	Sec	T. (S.)	R. (E.)	UTM E m	UTM N m	Unit	Lith.	SiO_2	TiO_2	Al_2O_3	Fe_2O_3	FeO	MnO	MgO	CaO	Na_2O	K_2O	P_2O_5	LOI (%)	Total (%)	Fe_2O_3T	Rb	Sr	Y	Zr	V	Ni	Cr	Nb	Ga	Cu	Zn	Co	Ba	La	Ce	U	Th	Sc	Pb	Yb	Be
1	92-26	20.2 ± 0.3	NE	SW	14	37	3	546460	4688530	Tmvhf	B	49.88	1.39	16.64	6.33	3.71	0.14	5.82	9.32	3.37	0.93	0.48	1.38	99.39	10.45	13.8	653	29	122	236	158	287	8	17.9	61	102	35	467	24	42	0.3	3.3	28	6.3	2.3	1.3
2	07SM-10	20.4 ± 0.3[a]	SW	SW	17	38	3	541290	4678510	Tmvhf	B	51.17	1.42	17.14	2.45	6.99	0.18	5.04	8.43	3.24	1.24	0.63	2.31	100.24	10.22	23	626	28	190	214	52	85	11	19.7	60	97	30	525	21	44	<0.5	1.8	22	6	--	--
3	00-62	21.10 ± 0.07[a]	SE	SW	19	37	4	549700	4686620	Tmvhf	B	51.50	1.21	17.49	8.05	2.24	0.13	4.17	8.83	3.44	0.82	0.38	1.76	100.02	10.54	9.2	749	22	122	215	94	212	7.5	19.7	52	100	28	421	17	36	1.1	1.4	28	5	--	--
4	92-41	19.5 ± 0.3	NW	NE	23	37	3	546820	4688070	Tmvhf	BA	52.29	0.91	18.11	3.96	4.30	0.13	5.28	8.97	3.12	1.00	0.24	1.21	99.52	8.74	11	859	21.4	73	212	53	133	5	22.2	72	76	33	365	17	26	0.7	3.3	23	7.7	1.4	1.2
5	92-24	20.5 ± 0.3	NE	SE	13	37	3	549060	4688670	Tmvhf	BA	53.79	0.89	17.27	3.19	4.93	0.13	5.54	7.97	3.58	1.09	0.30	1.11	99.79	8.67	23.4	643	24.8	120	181	67	161	4.5	20.6	29	76	20	619	26.7	62.1	2	6	20	6.3	--	--
6	91-61[1]	19.6 ± 0.3	NW	SW	7	37	4	549310	4690380	Tmvhf	BA	56.89	0.64	19.11	3.30	3.21	0.10	3.17	7.62	3.57	1.00	0.16	1.68	100.45	6.87	10.6	844	13	59	132	6	25	3.5	23.1	59	51	17	286	8	15	1	4	13	4.6	0.8	1.2
7	00-63	21.2 ± 0.3[a]	SE	SW	19	37	4	549700	4686710	Tmvhf	A	59.19	1.24	16.28	6.75	0.82	0.13	0.91	4.37	4.37	1.81	0.41	3.71	99.99	7.66	32.9	550	25.6	229	125	20	39	11.3	19.9	44	92	13	799	24	51	0.6	3.5	24	8	--	--
8	07SM-3	21.49 ± 0.10[a]	NE	SW	3	38	3	544690	4682380	Tmvhf	TrA	59.92	1.54	15.26	5.07	2.34	0.11	1.38	4.64	4.65	2.09	0.67	2.45	100.12	7.67	50.7	427	43.3	284	107	3	4	13.6	19.2	3	112	13	752	23	60	1.1	5.6	20	7	--	--
9	00-65	21.1 ± 0.3[a]	SE	SW	19	37	4	549730	4686840	Tmvhf	Rhy	69.36	0.67	14.79	3.17	0.37	0.05	0.23	1.27	5.65	2.79	0.07	1.27	99.69	3.58	50.9	231	42.9	365	46	5	10	19.2	21.6	3	84	3	896	28	44	2.7	4.4	11	12	--	--
10	SP02-18	--	NE	SW	19	37	4	549600	4687310	Tmvhf	B	47.46	1.06	15.65	5.02	5.32	0.18	9.66	9.93	2.90	0.52	0.45	1.81	99.95	10.93	5	599	15	76	256	185	623	9	20	99	101	48	387	21	38	<0.5	1.4	31	3	--	--
11	SP02-26	--	SE	SW	19	37	4	549770	4686550	Tmvhf	B	49.49	1.25	18.13	8.23	2.38	0.15	3.16	8.38	3.26	0.66	0.40	3.99	99.48	10.88	6.9	771	21	130	234	68	227	9.3	21.9	57	107	31	499	20	39	0.6	3.9	32	5	--	--
12	07SM-7	--	SW	SE	21	37	3	543520	4686530	Tmvhf	B	49.72	1.34	15.43	3.53	6.18	0.15	8.80	8.68	2.97	0.78	0.40	2.35	100.33	10.40	12.5	571	21.9	132	203	166	322	9.8	17.2	63	90	42	326	14	27	1.6	1.3	23	5	--	--
13	00-72	--	SW	SW	2	37	3	545900	4691320	Tmvhf	B	50.00	1.35	18.36	4.63	5.79	0.17	5.26	9.02	3.41	0.54	0.52	1.43	100.48	11.06	5.3	637	26.3	133	203	86	195	8.6	19	42	95	34	387	20	39	<0.5	2.6	24	6	--	--
14	92-42	--	NW	NE	23	37	3	546970	4687950	Tmvhf	B	50.38	1.41	16.91	6.77	3.44	0.14	4.74	9.29	3.32	0.93	0.48	2.12	99.93	10.59	14.8	643	28.1	140	229	155	308	10.5	19	57	101	25	439	23	46.8	0.8	1.2	26.9	7.3	2.3	1.3
15	SP02-29	--	NW	NE	24	37	3	548320	4687730	Tmvhf	B	50.73	0.89	18.84	8.51	0.97	0.07	1.90	5.70	2.00	0.42	0.11	10.08	100.21	9.59	8	689	12	101	120	52	135	6.2	20.3	77	75	18	321	12	33	<0.5	1.6	31	5	--	--
16	SP02-19	--	SE	SW	19	37	4	549660	4686760	Tmvhf	TrB	50.98	1.10	16.72	7.24	2.11	0.16	6.64	7.70	3.63	1.49	0.47	1.88	100.11	9.58	13.2	1165	19	115	182	136	258	6.5	21.1	81	90	36	727	20	42	1.1	3.6	23	5	--	--
17	07SM-8	--	SW	NE	17	38	3	542060	4679360	Tmvhf	B	51.20	1.37	16.85	7.89	2.50	0.18	5.58	8.20	3.36	1.17	0.59	1.33	100.22	10.67	18.8	615	26.9	177	218	56	121	9.6	19.1	40	102	34	554	19	46	<0.5	3.9	23	6	--	--
18	07SM-31	--	SW	NW	21	38	3	543050	4677740	Tmvhf	B	51.38	1.32	16.89	4.78	4.92	0.14	5.17	8.23	3.32	1.15	0.58	2.22	100.10	10.25	21.3	613	25.7	174	209	74	143	11.9	19.9	54	100	34	598	20	48	0.5	0.8	23	5	--	--
19	07SM-29	--	NE	SE	22	38	3	545670	4677510	Tmvhf	B	51.59	1.12	17.18	4.31	4.89	0.16	5.68	8.87	3.31	1.07	0.46	1.30	99.94	9.74	21.4	647	20.9	149	217	63	132	9.7	19.5	76	94	32	503	18	38	0.5	1	23	4	--	--
20	92-25	--	NE	SW	13	37	3	548260	4688680	Tmvhf	B	51.67	0.96	18.98	4.65	3.98	0.14	4.34	9.31	3.16	0.82	0.20	1.27	99.48	9.07	8.6	844	20	55	241	40	81	2.9	20	65	72	38	333	13	23	0.5	0.8	25	--	1.2	1.1
21	SP02-11	--	NW	NW	24	37	3	547660	4687820	Tmvhf	BA	52.01	0.90	18.46	4.99	4.01	0.13	4.56	8.45	2.85	0.97	0.24	2.97	100.55	9.45	10.1	793	16	104	214	69	141	5.6	21	58	88	31	387	17	34	1.1	2.8	25	5	--	--
22	07SM-13	--	NW	NW	15	38	3	544650	4679960	Tmvhf	BA	52.20	1.27	17.12	4.43	4.89	0.15	4.77	8.16	3.39	1.19	0.57	2.25	100.39	9.86	15.7	625	27.1	182	207	67	120	10.3	19.2	65	104	32	535	18	44	<0.5	1.1	24	7	--	--
23	07SM-9	--	SW	SE	15	38	3	545520	4678600	Tmvhf	BA	52.39	1.24	17.28	3.72	5.28	0.15	5.44	8.33	3.45	1.17	0.54	1.34	100.33	9.59	22.9	527	25.9	176	207	68	128	9.8	19.2	66	102	31	515	19	43	<0.5	1.3	23	6	--	--
24	SP02-10	--	NE	NE	23	37	3	547420	4687920	Tmvhf	BA	52.71	0.88	18.48	4.18	4.30	0.13	5.04	8.47	3.12	0.92	0.23	1.80	100.25	8.96	10.3	807	16	99	203	52	112	5.8	21	80	71	27	408	14	33	0.6	1.6	23	5	--	--
25	SP02-36	--	SW	NE	24	37	3	548470	4687670	Tmvhf	BA	52.72	1.56	18.76	8.52	0.67	0.06	0.53	5.13	3.93	0.98	0.51	5.69	99.04	9.26	14.8	633	32	203	157	8	20	11.7	23.6	44	89	11	689	29	53	0.5	4.4	33	6	--	--
26	00-69	--	NW	SE	12	37	3	548630	4690520	Tmvhf	BA	52.84	0.91	18.06	3.35	4.87	0.14	5.52	9.06	3.16	0.90	0.25	0.83	99.89	8.76	12.1	820	14.4	100	197	55	125	4.1	19.2	24	74	27	330	10	26	<0.5	1.2	25	6	--	--
27	07SM-12	--	W	NW	5	38	3	541450	4683060	Tmvhf	BA	53.68	0.85	18.16	3.86	3.92	0.12	4.72	7.94	3.06	1.45	0.17	2.11	100.04	8.22	29.9	659	19	119	204	40	61	2.2	18.5	37	78	26	310	12	22	<0.5	3.5	22	5	--	--
28	SP02-16	--	SW	NW	19	37	4	549200	4687550	Tmvhf	BA	53.76	1.09	18.94	2.93	4.35	0.13	4.31	8.07	3.36	0.83	0.21	2.02	99.98	7.76	8.1	511	40	132	223	34	100	7.4	21.6	54	84	30	585	23	37	0.8	3.8	30	6	--	--
29	00-68	--	NE	SE	12	37	3	549010	4690420	Tmvhf	BA	54.13	1.03	17.25	3.24	5.08	0.15	5.04	7.82	3.30	1.06	0.33	1.35	99.78	8.89	16.2	697	19	141	174	60	157	6.7	19.2	46	76	26	449	16	35	<0.5	1.4	20	7	--	--
30	00-71	--	NE	NE	11	37	3	547270	4691110	Tmvhf	BA	54.66	1.02	17.50	4.30	3.99	0.13	4.34	8.07	3.35	1.00	0.34	1.24	99.94	8.73	13.1	722	22.4	131	173	52	154	6.3	18.4	58	83	35	417	23	39	<0.5	0.7	25	6	--	--
31	SP02-24	--	SE	SW	19	37	4	549720	4686660	Tmvhf	BA	54.69	1.50	15.78	8.34	1.62	0.16	1.46	4.83	3.47	1.17	0.41	6.41	99.85	10.14	29.4	517	40	189	153	17	20	11.2	20.7	36	102	23	607	22	50	1.5	3	30	7	--	--
32	00-64	--	SE	SW	19	37	4	549720	4686760	Tmvhf	BA	55.23	1.28	16.99	8.22	0.67	0.15	1.33	4.86	3.72	1.51	0.40	5.57	99.93	8.96	26.8	547	24	183	149	31	60	9.6	19.9	35	90	20	676	20	45	1.9	2.2	25	8	--	--
33	07SM-4	--	NE	NE	29	37	3	542570	4686200	Tmvhf	BA	55.36	0.68	17.45	4.07	2.78	0.11	3.94	7.63	2.93	1.09	0.15	3.78	99.97	7.16	26	710	15.7	92	186	24	38	2.3	18.2	48	70	19	378	9	13	0.5	2.7	20	6	--	--
34	92-22	--	SW	NW	19	37	4	549130	4687500	Tmvhf	BA	55.41	1.10	17.82	2.41	4.13	0.12	4.20	8.08	3.58	1.13	0.22	0.93	99.13	7.00	20.6	521	32.6	119	218	27	109	4.7	19.3	56	82	31	536	16	29	--	1.8	26	--	2.4	1.1
35	SP02-4	--	SW	SE	11	37	3	546700	4689800	Tmvhf	BA	55.48	0.82	18.87	3.78	3.91	0.13	4.46	7.58	3.04	0.92	0.13	1.83	100.96	8.13	14.4	779	14	78	187	19	32	3.5	21.2	46	69	35	308	9	22	<0.5	1.4	20	4	--	--
36	SP02-28	--	NW	NE	24	37	3	548320	4687730	Tmvhf	BA	56.03	0.68	18.26	5.62	1.35	0.14	3.62	6.53	2.87	1.09	0.18	3.25	99.63	7.12	9	928	13	105	116	18	24	4.5	22	56	73	20	298	12	28	0.5	2.5	19	3	--	--
37	SP02-20	--	SE	NE	24	37	3	549060	4687500	Tmvhf	BA	56.74	1.08	17.44	2.94	3.94	0.11	3.86	7.60	3.58	1.21	0.23	1.28	100.01	7.32	26	524	31	133	223	33	94	7.4	20.1	53	83	25	482	20	35	<0.5	4.3	30	6	--	--
38	07SM-1	--	SE	SW	29	37	3	541700	4685050	Tmvhf	A	57.27	0.66	17.79	4.02	2.73	0.14	3.66	7.32	3.22	1.36	0.15	1.93	100.25	7.05	29.4	715	16.1	95	179	25	38	2.9	18.1	55	72	20	371	11	15	<0.5	3	19	6	--	--
39	SP02-22	--	NE	SW	19	37	4	549560	4687100	Tmvhf	A	59.10	1.11	14.79	4.99	1.46	0.08	0.90	3.17	2.38	1.57	0.23	11.04	100.81	6.61	31.1	399	39	244	81	8	18	14.8	20.1	19	98	10	816	24	54	0.6	3.9	23	9	--	--
40	07SM-2	--	NW	SE	4	38	3	543850	4682360	Tmvhf	TrA	59.41	1.60	15.54	5.91	1.82	0.12	1.11	4.69	4.64	2.03	0.70	2.75	100.32	7.93	45.1	442	65.3	280	112	2	5	13.3	19.4	11	117	16	735	26	65	1.7	5	23	13	--	--
41	SP02-23	--	NE	SW	19	37	4	549560	4687100	Tmvhf	A	60.92	1.22	14.40	4.16	1.19	0.06	0.94	2.50	2.56	1.57	0.21	11.23	100.97	5.48	30	393	29	276	88	4	10	16.9	21.3	18	73	10	811	36	67	1.7	4.8	21	12	--	--
42	07SM-6	--	NE	SW	21	37	3	543180	4686930	Tmvhf	D	63.83	0.40	14.15	2.73	0.67	0.03	0.87	1.47	3.12	3.70	0.08	9.01	100.06	3.47	68.7	155	49.4	395	34	2	10	23.8	19.8	7	74	2	875	41	90	1.7	6.7	10	13	--	--
43	00-66	--	SE	SW	19	37	4	549730	4686890	Tmvhf	Tr	66.94	0.65	14.29	1.60	1.59	0.11	0.49	1.48	3.78	4.21	0.12	4.35	99.61	3.37	57.3	224	46	357	47	4	11	18.7	20.4	5	86	4	1047	33	65	1.8	4.7	11	15	--	--
44	SP02-25	--	SE	SW	19	37	4	549750	4686740	Tmvhf	Tr	68.61	0.66	14.99	2.70	0.70	0.14	0.25	1.21	5.63	2.83	0.08	1.66	99.46	3.48	50.8	231	28	363	29	3	3	20.1	21.9	7	63	6	935	23	44	1.5	5.7	13	12	--	--
45	07SM-11B	--	NE	SE	29	37	3	542460	4685380	Tmvhf	Rhy	73.08	0.26	14.06	1.56	0.33	0.02	0.18	2.01	4.18	2.18	0.07	2.19	100.12	1.93	53.4	296	12.6	134	25	1	3	4.6	12.5	<2	32	<1	910	27	36	2	3.9	4	13	--	--
46	07SM-11A	--	NE	SE	29	37	3	542460	4685380	Tmvhf	Rhy	73.90	0.24	13.77	0.91	0.69	0.04	0.22	1.86	4.27	2.34	0.07	1.85	100.16	1.68	57.6	274	11.2	131	24	2	2	4.4	12	<2	37	<1	980	20	37	1.8	3.5	6	11	--	--
47	JB91-56[2]	5.35 ± 0.09	SW	SE	18	37	4	550220	4688240	Tmbpb	TrB	48.60	1.36	14.56	5.19	4.14	0.13	8.37	9.28	3.99	1.71	1.11	1.16	99.60	9.79	15.4	1718	21.6	105	220	97	242	16.7	24.5	86	118	36	905	55.4	93	2.1	8.2	21	5.4	1.3	2.3
48	92-21[3]	6.13 ± 0.10	NW	NW	19	37	4	549130	4687920	Tmbpb	TrB	49.62	1.06	15.41	5.58	3.11	0.13	7.83	9.25	3.33	2.16	0.63	1.56	99.67	9.04	21.3	2187	22.6	65	183	81	168	5.1	20.7	104	74	34.5	1749	43.8	92	2.4	7.9	18	9	1.3	--
49	SW21-91	--	SW	NW	18	37	4	549250	4688950	Tmbpb	TrB	48.86	1.35	14.57	5.16	4.17	0.13	8.26	9.25	4.40	1.79	1.10	1.59	100.63	9.79	16.3	1696	15.9	106	218	97	241	13.9	22.1	89	118	36	751	49	89	3.6	7.1	23	--	1.1	2.3

[1] Certain elements that were not measured in most of the other samples were measured in sample 91-61 (values in ppm) (Hf = 2.2, Ta 0.4, Nd = 10, Sm = 2.2, Eu = 0.82, Tb = 0.3, Lu = 0.16).

[2] Certain elements that were not measured in most of the other samples were measured in sample JB91-56 (values in ppm) (Hf = 3.4, Ta 0.6, Nd = 49, Sm = 6.47, Eu = 1.93, Tb = 0.6, Lu = 0.2).

[3] Certain elements that were not measured in most of the other samples were measured in sample 92-21 (values in ppm) (Hf = 2.9, Ta <0.3, Nd = 50, Sm = 8.87, Eu = 2.36, Tb = 0.8, Lu = 0.2).

(continued on next page)

Table 1 (page 2).

Map no.	Sample no.	K-Ar Age[a] Ma	1/4 of 1/4	1/4	Sec	T. (S.)	R. (E.)	UTM E m	UTM N m	Unit	Lith.	SiO_2	TiO_2	Al_2O_3	Fe_2O_3	FeO	MnO	MgO	CaO	Na_2O	K_2O	P_2O_5	LOI (%)	Total (%)	Fe_2O_3T	Rb	Sr	Y	Zr	V	Ni	Cr	Nb	Ga	Cu	Zn	Co	Ba	La	Ce	U	Th	Sc	Pb	Yb	Be
50	92-90	--	SW	SE	18	37	4	549970	4688480	Tmbpb	TrB	48.87	1.34	14.65	5.18	4.09	0.14	8.44	9.24	4.31	1.74	1.08	0.67	99.75	9.73	15.1	1777	11.6	171	246	111	246	18.3	20.9	87	149	32	705	26	85	1	5.5	19	4	--	--
51	00-74	--	NW	NE	19	37	4	550170	4688060	Tmbpb	TrB	49.77	1.27	14.79	4.74	4.34	0.14	8.16	8.98	4.10	1.73	1.03	0.83	99.88	9.56	17.3	1574	12.8	151	209	118	291	13.4	21	59	116	31	896	43	80	1.2	7.4	19	5	--	--
52	92-23	--	NW	SW	19	37	4	549130	4687320	Tmbpb	TrB	50.01	1.12	15.58	5.58	3.34	0.14	7.43	8.88	3.37	2.09	0.64	1.24	99.42	9.29	17.5	2290	30.5	53	220	87	262	4.9	18.4	110	72	35	1414	60	90	2.1	4.8	23	--	1.9	1.6
53	SP02-17	--	SW	NW	19	37	4	549320	4687400	Tmbpb	TrB	50.15	1.07	15.51	5.07	3.67	0.15	7.63	9.56	3.42	2.00	0.61	0.69	99.53	9.15	17.2	2310	20	120	192	99	236	5.5	19.9	86	74	33	1262	38	80	0.9	5.4	20	5	--	--
54	92-20	--	NE	NW	19	37	4	549730	4687970	Tmbpb	TrB	50.28	1.13	16.53	6.53	2.21	0.15	6.94	9.03	3.47	2.22	0.62	1.09	100.20	8.99	28.7	2243	24.6	163	228	60	128	6	15.9	85	89	22	1533	29	93	1.3	5.1	18	4	--	--
55	99-18	--	SW	NW	29	37	4	550950	4685830	Tmbpb	TrB	50.35	1.07	15.75	5.63	2.97	0.14	6.91	8.94	3.41	2.15	0.58	1.48	99.38	8.93	24.1	1827	18.1	109	217	68	177	6.6	21	91	77	29	1488	38	73	1.8	6.9	18	8	--	--
56	00-53	--	SW	NW	29	37	4	551000	4685910	Tmbpb	TrB	50.67	1.08	15.82	6.78	1.97	0.14	6.72	8.70	3.25	2.18	0.58	1.54	99.43	8.97	28.4	1752	20	129	195	80	191	4.6	18.9	82	84	31	1682	38	79	2.6	6.1	20	7	--	--
57	00-42	--	SE	NW	29	37	4	551210	4685950	Tmbpb	TrB	50.70	1.06	15.22	5.65	2.97	0.15	7.32	9.68	3.21	2.31	0.62	0.72	99.61	8.95	30.2	2209	23.7	137	179	88	198	8.9	17.4	100	77	31	2199	44	108	2.1	10	18	13	--	--
58	94-40	5.43 ± 0.18	NW	NE	35	37	3	546820	4684510	Tmbab	B	49.10	0.66	13.45	2.81	6.52	0.14	15.59	8.21	2.28	0.51	0.12	0.83	100.22	10.06	4.8	804	13.7	30	182	263	879	1.3	15.5	69	71	47	138	9	21	--	--	29	--	1.7	0.8
59	94-42	5.54 ± 0.15	NW	SE	31	37	4	549990	4683970	Tmbab	B	51.82	1.05	17.54	6.75	2.28	0.14	5.88	7.98	3.78	1.10	0.35	1.65	100.32	9.28	9	1392	19	56	158	135	194	4.7	23.2	43	76	18	506	15.2	39.3	1.8	6.5	19	3.9	2.2	1.3
60	07SM-16	5.99 ± 0.04[a]	NW	NE	2	38	3	546800	4682950	Tmbab	BA	53.53	0.96	16.71	3.77	3.87	0.13	7.11	8.86	3.60	0.86	0.30	0.59	100.29	8.07	4.8	1265	12.6	110	188	72	143	2.1	18.9	32	70	28	270	15	25	1	1.7	18	4	--	--
61	RSP94-94	5.73 ± 0.15	SE	SW	20	37	4	551370	4686920	Tmbab	BA	53.71	1.16	17.38	3.23	4.92	0.15	4.83	8.00	3.96	1.19	0.48	0.91	99.92	8.70	10.4	968	24.5	132	170	34	74	7.8	21.7	37	70	25	523	19	43.9	0.9	1.2	20	5	2.4	1.2
62	07SM-21	--	SW	NE	35	37	3	546800	4684330	Tmbab	B	48.78	0.66	13.10	2.17	7.96	0.16	15.85	7.84	2.01	0.43	0.13	0.94	100.03	11.02	2.3	801	10.4	70	190	355	990	1.5	14.3	77	87	62	103	10	14	<0.5	1.3	24	3	--	--
63	07SM-20	--	NE	NW	35	37	3	546700	4684710	Tmbab	B	49.21	0.68	13.43	2.51	7.49	0.15	15.09	7.92	2.02	0.42	0.13	1.32	100.37	10.83	1.6	807	11.8	70	194	315	890	2.1	15.5	72	85	58	103	11	15	<0.5	<0.5	23	3	--	--
64	00-43	--	SE	NW	29	37	4	551180	4685980	Tmbab	B	49.65	1.47	16.81	7.29	4.03	0.15	5.02	8.51	3.14	0.76	0.40	2.44	99.67	11.77	11.4	518	28.7	129	208	93	208	8.6	18.9	59	97	32	493	13	32	<0.5	1.8	26	3	--	--
65	07SM-26	--	SE	SW	32	37	4	551250	4683720	Tmbab	B	49.74	0.74	15.89	2.52	6.47	0.15	9.56	10.16	2.54	0.67	0.26	1.47	100.17	9.71	6.6	602	14.1	82	245	161	625	6	17.3	68	81	39	402	17	30	<0.5	1.9	32	3	--	--
66	07SM-19	--	SE	NE	36	37	3	548870	4684420	Tmbab	B	51.02	1.06	16.51	3.22	5.17	0.14	8.15	9.34	3.26	1.07	0.42	0.72	100.08	8.97	14.7	962	19.1	140	231	103	275	5.2	18.9	84	91	34	563	20	42	0.5	3.5	25	4	--	--
67	94-41	--	NE	NW	6	38	4	549570	4683220	Tmbab	B	51.24	1.11	16.49	1.20	7.13	0.13	7.65	9.28	3.41	1.21	0.45	0.93	100.23	9.12	16.9	1006	21.2	105	227	89	245	5.6	18.7	73	86	19	729	--	58	<0.5	3.1	29	--	2.3	1.6
68	00-48	--	SW	SE	30	37	4	549950	4685120	Tmbab	B	51.82	0.94	16.77	4.47	3.50	0.13	6.36	8.61	3.75	1.19	0.38	0.66	98.58	8.36	10	1520	17.6	104	190	103	186	7.4	20.8	77	74	32	478	22	48	1.6	3.7	22	6	--	--
69	00-47	--	SW	SW	29	37	4	550730	4685230	Tmbab	B	51.86	0.86	18.66	2.52	5.55	0.14	5.23	9.50	3.43	0.69	0.17	0.71	99.32	8.69	3.8	1053	13.3	75	187	97	382	5.1	18.1	113	69	42	189	7	17	<0.5	3	26	5	--	--
70	00-49	--	NW	NW	31	37	4	549110	4684770	Tmbab	BA	52.46	0.94	16.95	4.46	3.49	0.12	6.28	8.32	3.67	1.16	0.36	1.15	99.36	8.34	11.8	1365	15.6	103	188	113	177	3.5	20.3	72	82	29	480	22	46	0.9	2.2	21	4	--	--
71	00-46	--	SE	NW	32	37	4	551320	4684390	Tmbab	BA	52.71	0.86	18.64	3.35	4.73	0.14	5.26	9.62	3.33	0.69	0.18	0.56	100.07	8.61	3.4	1041	13.2	75	208	22	64	3.5	19.8	64	70	27	214	10	20	0.6	<0.5	24	3	--	--
72	94-39	--	NW	NW	1	38	3	547740	4682940	Tmbab	BA	52.82	0.86	18.17	3.94	4.51	0.14	5.46	9.90	3.17	0.73	0.16	0.80	100.66	8.95	6.5	1044	16	39	230	20	53	1.3	19.1	123	72	19	199	--	23	<0.5	<0.5	31	--	1.9	1.2
73	07SM-18	--	NE	SW	36	37	3	548030	4683890	Tmbab	BA	52.83	0.99	17.54	4.26	3.73	0.13	6.07	8.35	3.85	1.16	0.35	0.85	100.11	8.41	9.7	1460	18.1	124	192	95	131	2.9	21.5	46	89	29	490	18	36	0.8	2.2	19	5	--	--
74	00-50	--	SE	NE	31	37	4	550470	4684170	Tmbab	BA	53.22	1.00	17.03	5.13	2.87	0.14	5.98	7.84	3.75	1.24	0.35	0.97	99.52	8.32	12.1	1343	16.8	110	175	119	164	3.6	20.4	56	83	28	479	21	40	2	3.7	20	3	--	--
75	07SM-14	--	NW	NE	15	38	3	545360	4679870	Tmbab	BA	53.13	1.14	17.90	4.48	4.48	0.12	3.43	7.22	3.85	1.23	0.50	2.54	100.02	9.46	12.1	785	42.3	149	202	37	46	6.6	20.7	48	85	29	458	27	40	<0.5	0.5	20	5	--	--
76	07SM-15	--	SW	NW	14	38	3	546030	4679560	Tmbab	BA	53.54	1.12	17.79	4.62	4.40	0.14	3.56	7.62	3.92	1.22	0.50	1.83	100.26	9.51	12.4	825	31.3	152	199	34	42	7.3	20.3	52	84	28	447	21	37	<0.5	1.7	19	4	--	--
77	00-52	--	SW	NW	29	37	4	550870	4685820	Tmbab	BA	54.25	1.13	17.48	3.09	4.84	0.15	4.48	7.82	3.99	1.20	0.52	0.47	99.42	8.47	10.8	850	24.2	143	177	33	72	7.4	21.3	56	80	22	486	21	39	<0.5	0.5	22	5	--	--
78	00-41	--	SE	NW	29	37	4	551380	4685930	Tmbab	BA	54.27	1.13	17.35	2.76	5.15	0.14	4.55	7.86	3.95	1.19	0.50	0.74	99.59	8.48	6.7	923	27.5	143	165	39	59	9.8	19.2	67	74	25	524	24	49	0.6	<0.5	19	4	--	--
79	07SM-22	--	SW	SW	6	38	4	549450	4681820	Tpbmp	B	48.55	1.09	16.01	4.20	5.47	0.16	9.37	10.07	3.21	0.60	0.47	0.86	100.06	10.28	5.5	787	15.2	95	259	121	415	6.8	19.4	97	112	42	279	18	31	0.8	2.4	32	4	--	--
80	07SM-25	--	NE	NW	5	38	4	551480	4682970	Tpbmp	B	48.79	1.15	15.06	5.45	4.15	0.14	9.70	8.71	3.29	1.13	0.75	1.79	100.11	10.06	11.3	1135	12.8	152	228	177	410	16.1	21.7	73	113	39	555	27	59	<0.5	4.2	21	3	--	--
81	07SM-17	--	NE	SW	1	38	3	547960	4682360	Tpbmp	B	49.72	0.71	15.08	2.72	6.63	0.16	10.42	10.11	2.47	0.64	0.25	1.13	100.04	10.09	6.7	607	14	95	245	180	625	3.8	16.4	78	88	41	260	15	21	0.9	2.9	32	3	--	--
82	07SM-27	--	NW	NE	8	38	4	551530	4681460	Tpbmp	B	49.88	1.16	16.42	3.16	5.87	0.15	8.30	9.04	3.26	1.10	0.50	1.45	100.29	9.68	14	890	24.5	148	227	95	295	9	21	72	92	36	805	27	57	<0.5	4.7	25	3	--	--
83	06SM-63	--	SE	NW	13	38	3	548000	4679570	Tpbmp	B	50.02	1.16	15.84	3.36	5.27	0.14	8.22	9.04	3.20	1.26	0.57	2.24	100.32	9.22	24.2	930	17.5	161	222	100	257	10.1	19.5	75	100	38	770	21	63	1.2	5.9	26	5	--	--
84	07SM-23	--	NW	NE	18	38	4	550250	4680010	Tpbmp	B	50.04	0.94	15.37	3.68	5.56	0.16	10.60	9.08	3.02	0.61	0.25	0.89	100.20	9.86	6.4	759	29.8	90	220	275	540	4.1	17.8	50	90	46	295	16	23	<0.5	1.8	26	4	--	--
85	07SM-28	--	NW	NW	8	38	4	551040	4681700	Tpbmp	B	50.07	0.74	15.18	5.19	4.15	0.16	10.28	9.54	2.55	0.78	0.27	1.49	100.40	9.80	11	622	14.4	82	234	215	675	6.3	16.2	73	88	45	455	18	30	<0.5	1.5	29	3	--	--
86	94-38	--	SW	SW	1	38	3	547840	4681760	Tpbmp	B	50.69	0.72	15.77	2.78	6.08	0.15	9.07	10.27	2.63	0.70	0.24	1.33	100.43	9.54	10.1	575	23.3	65	236	134	522	4.1	16	74	79	26	365	--	37	0.9	1.8	38	--	2.7	1.2
87	07SM-24	--	NE	SW	17	38	4	551290	4679010	Tpbmp	B	50.85	1.13	16.49	3.36	5.47	0.15	7.86	8.79	3.21	1.12	0.45	1.22	100.10	9.44	13.9	945	29.2	133	221	118	264	8	19	108	84	34	872	21	39	0.9	2	24	3	--	--
88	03SM-55	--	SW	SE	18	38	4	550120	4678560	Tpbmp	B	51.37	1.09	16.38	3.60	5.07	0.14	7.15	9.31	3.11	0.99	0.39	1.04	99.64	9.23	15.5	859	22.4	108	206	82	226	5.4	20.3	68	74	32	674	25	54	1	4.1	23	5	--	--
89	06SM-62	--	SE	NW	19	38	4	549840	4677750	Tpbmp	B	51.51	1.10	16.52	2.95	5.38	0.14	7.66	9.12	3.19	1.12	0.46	1.18	100.33	8.93	14.3	1053	23.5	141	221	104	212	7.1	18.9	82	89	36	713	20	50	0.6	1.5	25	6	--	--
**	03SM-57	--	SW	NW	28	38	4	552800	4676070	Tpbbm	B	50.59	1.04	17.24	3.51	5.65	0.16	7.31	9.56	2.82	0.59	0.21	1.23	99.91	9.79	8.8	564	21.2	80	213	93	328	3.8	17.7	66	69	36	322	12	24	<0.5	1.4	28	5	--	--
**	06SM-60	--	SW	SE	29	38	4	551760	4675630	Tpbbm	B	51.18	1.06	17.40	3.13	5.71	0.15	7.60	8.45	3.29	0.60	0.26	1.24	100.07	9.48	8.9	614	21.9	98	185	141	329	3.7	17.5	56	82	39	309	11	24	<0.5	1.1	25	5	--	--
**	03SM-56	--	NW	NE	29	38	4	551910	4676760	Tpbbm	B	51.93	1.06	16.78	1.96	6.77	0.16	7.83	8.19	3.21	0.60	0.26	0.73	99.48	9.48	10	561	21.5	98	170	138	316	4.3	18.3	62	69	35	317	14	30	<0.5	1.1	25	5	--	--
90	00-67	0.36 ± 0.06[a]	SE	SW	19	37	4	549640	4686930	Qbrb	B	51.61	0.90	17.34	2.08	5.77	0.15	7.37	10.25	2.92	0.41	0.15	0.76	99.71	8.49	5.1	860	18.7	85	194	81	293	2.4	18.1	76	62	31	157	11	27	<0.5	1.5	31	3	--	--
91	SP02-21	--	SE	NW	19	37	4	549610	4687360	Qbrb	B	50.69	0.89	17.27	2.10	5.92	0.15	7.71	10.19	2.83	0.32	0.15	1.17	99.40	8.68	2.5	855	18	85	202	73	267	4	19.2	69	62	34	216	14	30	<0.5	2.2	32	3	--	--
92	84-15	--	NW	SW	8	37	4	551020	4690230	Qbrb	B	50.73	0.95	17.79	8.08	0.63	0.15	6.93	9.83	3.06	0.42	0.17	1.33	100.07	8.78	2	825	19.4	81	194	64	178	2.6	15.4	56	89	29	145	10	21	<0.5	0.6	30	1	--	--
93	00-73	--	NE	NE	19	37	4	550340	4688060	Qbrb	B	51.15	0.90	17.55	1.61	6.32	0.15	7.11	10.42	2.87	0.37	0.14	1.12	99.71	8.63	4.80	814	19.9	81	206	66	251	2.2	17.3	62	67	31	153	12	22	<0.5	0.8	32	4	--	--
94	00-70	--	NE	NW	13	37	3	547920	4689660	Qbrb	B	51.16	0.88	17.22	2.92	5.26	0.15	7.99	10.00	2.70	0.33	0.15	1.44	100.20	8.77	3.80	878	18.3	82	198	109	358	2	17	72	64	35	169	14	25	1.1	<0.5	32	4	--	--
95	SP02-3	--	SE	SE	11	37	3	547140	4689940	Qbrb?	B	51.16	0.88	16.82	2.60	5.79	0.16	8.87	10.11	2.72	0.39	0.17	0.99	100.65	9.03	3.8	858	17	86	205	129	383	4.1	18.1	66	66	39	170	8	23	<0.5	2.8	34	2	--	--
***	91-42	--	NW	SW	4	38	4	552700	4682380	Qbbb	B	48.41	1.03	16.97	2.79	6.90	0.16	8.96	10.19	2.53	0.20	0.13	1.68	99.95	10.46	1.6	665	26.1	54	231	133	380	2.4	17.2	89	65	35	148	--	25	1.6	--	39	--	--	--
***	HP94-67	--	NW	NW	10	38	4	554060	4681330	Qbbb	B	48.71	0.91	17.95	2.89	5.93	0.17	9.06	10.00	2.45	0.24	0.12	1.97	100.40	9.48	2.5	638	21.7	62	215	108	378	3.6	17.8	53	61	32	137	10.8	23.8	1.4	1.6	29.9	5	--	--
***	99-15	--	SW	SW	4	38	4	552570	4681940	Qbbb	B	48.96	0.92	17.64	2.39	6.28	0.16	9.11	10.54	2.57	0.21	0.12	1.65	100.55	9.37	0.8	649	19.2	58	224	150	417	4.2	19.1	84	62	40	132	5	19	1.1	4.1	32	3	--	--
96	SP02-12	--	NW	NE	23	37	3	547000	4687800	Qls	B	47.31	1.37	18.82	7.23	4.23	0.19	5.04	9.62	3.06	0.45	0.49	2.65	100.45	11.93	4.8	597	26	147	215	102	358	11	21.3	67	93	40	525	24	46	<0.5	3.9	33	6	--	--
97	95-36	--	SE	NE	22	37	3	545790	4687520	Qls	B	48.50	1.34	16.66	4.24	5.65	0.15	7.21	9.13	3.20	0.68	0.33	3.08	100.17	10.52	10.00	524	19.5	102	198	120	238	7.5	18.4	56	84	36	296	15.3	31.6	1.4	1.5	24	5.2	--	--
98	95-37	--	SE	NE	22	37	3	545730	4687450	Qls	B	49.01	1.33	16.84	2.80	6.77	0.16	7.77	8.90	3.29	0.73	0.33	2.32	100.25	10.32	11.50	538	19.7	102	187	128	257	7.7	18.2	55	79	33	324	12.4	27.7	0.9	0.8	24.8	5.2	--	--
99	SP02-2	--	NE	SE	15	37	3	545680	4688760	Qls	B	49.06	1.41	17.82	8.97	2.47	0.19	4.74	8.80	3.08	0.68	0.46	3.07	100.76	11.72	7.3	583	27	137	235	149	364	10.7	21	65	104	48	493	22	46	<0.5	3.3	31	6	--	--
100	SP02-14	--	NE	SW	23	37	3	546520	4687280	Qls	B	49.53	1.48	18.02	9.48	1.95	0.18	4.14	8.76	3.06	0.94	0.52	2.75	100.79	11.65	14.7	591	26	146	230	116	344	11.5	21.2	69	109	45	548	24	49	<0.5	3.1	31	6	--	--
101	SP02-5	--	NE	SE	15	37	3	545640	4688730	Qls	B	49.71	1.40	17.20	9.46	2.05	0.20	4.52	8.90	3.08	0.84	0.45	2.39	100.20	11.74	13.2	591	30	141	219	154	347	10.7	20.7	64	97	46	459	25	43	1.3	2.6	30	6	--	--
102	SP02-27	--	NE	SE	24	37	3	548900	4687130	Qls	B	50.68	1.28	17.54	8.31	2.24	0.12	3.50	8.29	3.44	0.78	0.39	3.31	99.88	10.80	8.1	675	20	125	220	93	171	9.3	21	53	92	26	443	15	39	<0.5	2.7	31	4	--	--
103	07SM-5	--	SE	SE	17	37	3	542300	4688470	Qls	BA	52.79	1.00	17.34	3.82	4.13	0.13	6.34	8.62	3.75	1.07	0.35	0.85	100.19	8.41	8.6	1415	16.9	127	198	98	119	4	20.8	120	84	30	470	13	33	1.2	<0.5	20	5	--	--

** These samples are not from within the Robinson Butte 7.5' USGS quadrangle, but were collected in the southeasterly-adjacent Little Chinquapin Mtn. 7.5' quadrangle. They were included in this data table as examples of the Tpbbm unit's geochemistry, which would not be otherwise represented.

*** These samples are not from within the Robinson Butte 7.5' USGS quadrangle, but were collected in the easterly-adjacent Brown Mountain 7.5' quadrangle. They were included in this data table as examples of the Qbbb unit's geochemistry, which would not be otherwise represented.

(continued on next page)

Table 1 (page 3).

Map no.	Sample no.	K-Ar Age(a) Ma	1/4 of 1/4	1/4	Sec	T. (S.)	R. (E.)	UTM E m	UTM N m	Unit	Lith.	SiO_2	TiO_2	Al_2O_3	Fe_2O_3	FeO	MnO	MgO	CaO	Na_2O	K_2O	P_2O_5	LOI (%)	Total (%)	Fe_2O_3T	Rb	Sr	Y	Zr	V	Ni	Cr	Nb	Ga	Cu	Zn	Co	Ba	La	Ce	U	Th	Sc	Pb	Yb	Be
104	SP02-8	--	NW	SE	15	37	3	545090	4688570	Qls	BA	53.18	0.90	18.23	5.38	2.12	0.10	3.43	9.76	3.28	1.01	0.21	2.47	100.07	7.74	7	1086	16	99	252	35	73	4.1	22.1	70	76	27	377	16	30	0.7	2.9	28	2	--	--
105	SP02-32	--	NW	SE	24	37	3	548610	4687230	Qls	BA	53.26	0.78	18.95	4.67	3.49	0.13	3.95	8.48	3.20	0.76	0.13	1.59	99.39	8.55	7.1	770	13	62	200	31	57	3.8	21.4	66	68	25	280	11	20	<0.5	2.2	26	3	--	--
106	95-35	--	SE	SE	15	37	3	545670	4688330	Qls	BA	53.49	0.88	18.77	6.04	2.70	0.11	4.13	8.24	2.97	0.91	0.12	2.06	100.42	9.04	10.1	850	12.8	63	196	25	26	3	20.8	22	66	22	229	9.6	20	0.4	0.2	22.4	5.1	--	--
107	SP02-13	--	SE	NW	23	37	3	546590	4687440	Qls	BA	54.23	0.84	19.00	6.56	1.42	0.13	4.64	8.49	3.03	0.86	0.13	1.28	100.59	8.14	9.7	856	12	77	197	21	42	3.8	21.3	45	68	25	228	8	18	<0.5	3.1	24	4	--	--
108	SP02-6	--	NW	SE	15	37	3	545380	4688690	Qls	BA	54.27	0.86	19.36	7.35	0.78	0.13	4.19	8.00	2.97	0.77	0.13	1.85	100.66	8.22	9.3	823	14	80	175	15	29	3.9	21.3	41	74	26	251	9	19	<0.5	2.3	22	4	--	--
109	SP02-7	--	NW	SE	15	37	3	545290	4688620	Qls	BA	54.41	0.85	19.09	4.62	3.03	0.12	3.92	8.25	2.88	0.93	0.13	2.03	100.27	7.99	12.4	847	13	80	206	13	32	3.7	21.4	51	74	28	256	9	21	<0.5	1.2	23	5	--	--
110	SP02-31C	--	SW	NE	24	37	3	548290	4687660	Qls	BA	56.17	0.65	18.33	4.76	1.38	0.06	2.77	6.35	3.21	1.00	0.17	5.38	100.22	6.29	8	985	10	94	160	17	28	3.9	20.9	43	57	18	276	11	28	0.9	0.7	18	3	--	--
111	SP02-31B	--	SW	NE	24	37	3	548290	4687660	Qls	BA	56.28	0.65	18.31	4.72	1.42	0.06	2.76	6.38	3.22	0.99	0.17	5.48	100.45	6.30	8.5	992	10	98	160	17	23	3.8	21.2	44	58	17	275	8	23	<0.5	2.7	20	3	--	--
112	SP02-33	--	SW	NE	24	37	3	548290	4687660	Qls	BA	56.38	0.65	18.96	4.95	1.80	0.08	2.41	6.81	3.37	0.93	0.16	2.85	99.35	6.95	7.2	1069	10	98	154	18	23	3.8	21.6	56	65	17	238	11	26	0.7	2.2	20	3	--	--
113	SP02-30	--	SW	NE	24	37	3	548360	4687620	Qls	BA	56.73	0.67	17.55	4.33	2.60	0.13	3.73	6.71	2.85	1.37	0.17	2.63	99.45	7.22	9.7	988	11	101	133	18	32	4.3	21.1	57	61	18	285	8	23	1	1.3	16.4	4	--	--
114	SP02-31A	--	SW	NE	24	37	3	548290	4687660	Qls	BA	56.75	0.65	18.14	4.62	1.54	0.06	2.78	6.32	3.18	0.99	0.16	5.42	100.62	6.33	8.8	986	10	96	159	17	28	3.9	20.6	43	57	18	277	11	25	0.5	2.8	19	3	--	--
115	SP02-34	--	SW	NE	24	37	3	548290	4687660	Qls	BA	56.92	0.65	19.01	4.00	2.43	0.09	2.75	7.16	3.43	0.95	0.16	2.06	99.62	6.70	6.5	1098	11	98	148	19	23	3.8	22.3	44	60	20	238	11	24	<0.5	3	21	2	--	--
116	SP02-35	--	SW	NE	24	37	3	548570	4687480	Qls	A	59.64	1.19	14.46	4.92	1.71	0.12	0.77	2.32	2.19	1.73	0.17	11.22	100.42	6.82	39.3	488	42	238	59	3	5	14.1	20.2	15	96	9	859	27	53	1.2	4	21	9	--	--
117	SP02-15	--	NE	SE	22	37	3	545740	4687230	Qls	A	59.65	0.67	17.57	4.11	1.99	0.09	2.46	6.25	3.63	1.52	0.20	2.54	100.67	6.32	30.3	657	16	124	120	14	25	6.1	19.6	43	62	16	487	11	26	1.8	4	16	14	--	--
118	95-38	--	SW	NE	22	37	3	545460	4687540	Qls	A	59.67	0.81	17.46	5.49	0.92	0.10	1.21	5.13	4.14	1.66	0.19	3.23	100.01	6.51	33.1	615	16.9	116	101	14	13	5.6	18.9	24	58	9	768	14.9	37.9	1.2	4.6	18.2	10.2	--	--
119	95-39	--	SW	NE	22	37	3	545460	4687540	Qls	A	59.81	0.93	17.09	5.09	1.82	0.10	2.14	5.79	4.25	1.51	0.19	1.94	100.66	7.11	30.9	496	17.9	120	180	7	21	5.5	19	31	69	13	485	11.8	34	0.8	3.5	20.5	8.6	--	--
120	SP02-1	--	NW	NW	17	37	3	541340	4689650	Qls	A	60.59	0.99	15.99	2.43	3.63	0.13	2.22	5.64	3.58	1.62	0.27	3.28	100.35	6.46	63.6	413	23.6	140	168	5	11	6.9	19.3	26	77	15	490	16	33	1.9	2.8	21	8	--	--